GEOLOGICA CARPATHICA, OCTOBER 2006, 57, 5, 379–396

Upper mantle xenoliths from the Pliocene Kozákov volcano (NE Bohemia): P-T-f_{O_2} and geochemical constraints

PATRIK KONEČNÝ[1], JAROMÍR ULRYCH[2], PAVEL SCHOVÁNEK[3], MONIKA HURAIOVÁ[4] and ZDENĚK ŘANDA[5]

[1]Geological Survey of the Slovak Republic, Mlynská dolina 1, 817 04 Bratislava, Slovak Republic; konecnyp@gssr.sk
[2]Institute of Geology, Academy of Sciences of the Czech Republic, Rozvojová 269, 165 02 Praha 6, Czech Republic
[3]Czech Geological Survey, Klárov 131/3, 118 21 Praha 1, Czech Republic
[4]Comenius University, Department of Mineralogy and Petrology, Mlynská dolina, 842 15 Bratislava, Slovak Republic
[5]Nuclear Physics Institute, Academy of Sciences of the Czech Republic, 250 68 Řež, Czech Republic

(Manuscript received November 9, 2004; accepted in revised form October 6, 2005)

Abstract: Upper mantle xenoliths are abundant in the basanites of the Pliocene Kozákov volcano. The studied samples of spinel lherzolites come from the depth of about 50–75 km. Their mineral assemblage preserved subsolidus temperatures of 1165–1052 °C from the time of xenolith entrapment. Oxygen fugacity varies from +0.14 to +0.93 log unit relative to fayalite-magnetite-quartz (FMQ) buffer. Major bulk-rock oxides and variations in mineral chemistry indicate a continual depletion trend mainly associated with extraction of basaltic melt from the mantle. Mineralogical features and the absence of highly oxidized lherzolites suggest a negligible degree of modal metasomatic overprint. On the contrary, the LREE upward patterns and U-shaped REE patterns of clinopyroxenes, as well as of the bulk lherzolite compositions are indicators of cryptic metasomatic event(s) in the upper mantle. The U-shape REE patterns corroborates to enrichment mechanisms in the mantle by reactive porous flow and chromatographic fractionation. A possible cryptic metasomatic event(s) could have occurred in pre-Cenozoic times, probably during the Variscan orogeny.

Key words: Bohemian Massif, Cenozoic volcanism, ultramafic xenoliths, spinel lherzolite, harzburgite, peridotite.

Introduction

The young continental intraplate volcanism (Upper Cretaceous to Quaternary) of the Bohemian Massif forms an integral part of the Central European Volcanic Province. The origin and distribution of the volcanism are controlled by WSW–ENE-oriented tectonic systems related to the Ohře/Eger Rift and by the WNW–ESE Labe Tectono-volcanic Zone (Fig. 1). On the basis of radiometric ages and geochemical signatures, Ulrych & Pivec (1997) and Ulrych et al. (1999) defined two series of intraplate alkaline volcanisms in the Bohemian Massif: (i) a pre-rift unimodal ultramafic (79–49 Ma) and (ii) a rift-related bimodal volcanism (42–0.26 Ma).

Even though mantle xenoliths of the peridotite–pyroxenite series are abundant in young volcanics of the Bohemian Massif (more than 100 occurrences have been reported, see Ulrych & Adamovič 2004), they have still not been systematically studied (cf. Jakeš & Vokurka 1987).

Ultramafic xenoliths from basanitic lava flows of the Kozákov volcano, situated in the Labe Tectono-volcanic Zone (Fig. 1), NE Bohemia, were studied by Fediuk (1971), Vokurka & Povondra (1983), Vokurka & Kober (1993), Medaris et al. (1997, 1999) and Christensen et al. (2001). The lava flows are widely known by the presence of frequent and large ultramafic xenoliths. Farský (1876) already published the very first chemical analyses of olivine, orthopyroxene, clinopyroxene and spinel of the Kozákov lherzolite xenoliths, thereby preceding the general interest in mantle-derived materials by about one century. The recent studies on lherzolite xenoliths from the Kozákov volcano documented two textural types of xenoliths: (i) medium-grained equigranular and (ii) coarse-grained protogranular, crystallized at 975–1090 °C and 1.20–1.86 GPa (Medaris et al. 1997). Studies on ultramafic xenoliths from other regions of the Bohemian Massif were presented by Fediuk & Fediuková (1989), Frýda & Vokurka (1995) and Ulrych et al. (2000).

The upper mantle beneath the Central European Volcanic Province reveals (i) vertical and lateral heterogeneities (cf. Babuška & Plomerová 1988) and (ii) metasomatic influence (Lloyd 1987; Wilson & Downes 1991; Wedepohl et al. 1994; Wilson et al. 1994; Downes 2001). These variations commonly correspond to the enrichment/depletion of upper mantle lherzolite in incompatible elements as reported, by Wedepohl (1987), Downes (2001), Downes et al. (1992), and Wedepohl et al. (1994) from the Central European and the Western European Volcanic Provinces.

Based on textural and geochemical evidence, Lloyd & Bailey (1975) postulated a metasomatic transition between spinel lherzolite and alkali clinopyroxenite (clinopyroxene + titaniferous phlogopite ± titanian magnetite, apatite, titanite and rare corroded olivine) for the xenolith suites from the rift valley volcanics of the West Eifel and Uganda. It has been suggested that metasomatism is either a necessary precursor to magmatism (Lloyd & Bailey 1975; Wass & Rogers 1980; Witt-Eickschen & Kramm 1998) or a consequence of alkali basaltic magmatism (Wilshire et al. 1980; Menzies et al. 1985). The likely connection between the origin of alkali

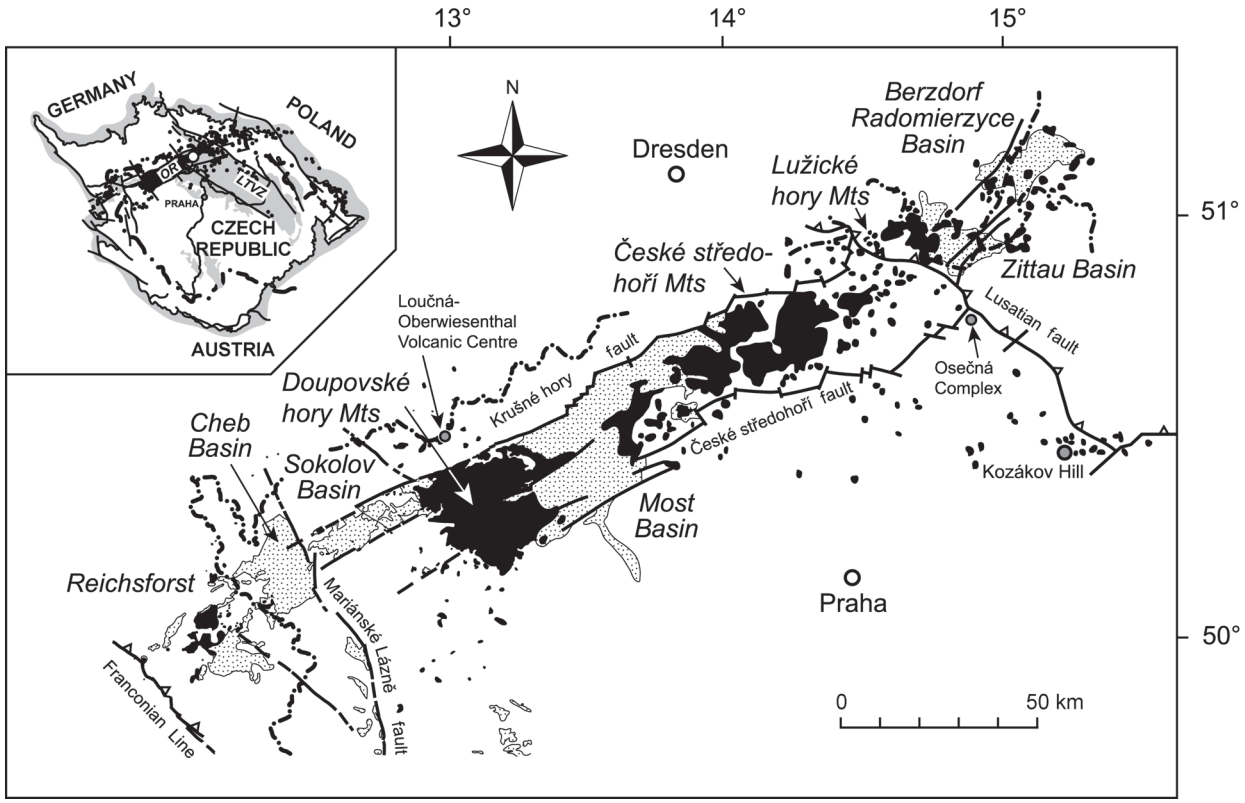

Fig. 1. A tectonic sketch of the Bohemian Massif and the main Cenozoic tectonic structures, volcanic and sedimentary deposits (modified after Christensen et al. 2001).

clinopyroxenite xenoliths and intrusive alkali complexes was emphasized by Upton (1967), Lloyd & Bailey (1975, 1994) and Erickson et al. (1985). These authors considered them manifestations of the same igneous processes. Compared with the original lherzolite mantle, pyroxenite xenoliths indicate enrichment in incompatible and large ion lithophile elements, and the host lavas are thought to be indicative of the rheomorphic metasomatized mantle (Lloyd & Bailey 1975).

Seismological data indicate a total lithosphere thickness of 80–140 km beneath the Bohemian Massif, of which about 70–80 km are possibly formed by highly anisotropic olivine-rich mantle lithosphere (Babuška & Plomerová 1988; Plomerová et al. 1998).

Variations in the upper mantle composition beneath the Bohemian Massif can be deduced from geochemical data on peridotite mantle xenoliths in the above mentioned Cenozoic volcanic rocks. Peridotite mantle xenoliths in the Bohemian Massif are free of K-, OH-, F-bearing phases from the supposedly metasomatized mantle. Using Sr isotopic data, Frýda & Vokurka (1995) mentioned carbonate metasomatism in a lherzolite xenolith from a basanite flow of the central part of the České středohoří Mts. Phlogopite and Mg-hastingsite were described by Kramer & Seifert (2000) in dunite xenoliths from the Cenozoic basaltic rocks of the Elbe Zone, Saxony. Lherzolite–harzburgite xenoliths in basanite dykes of the České středohoří Mts and basanite intrusion at Plesý Hill in the Lužické hory Mts (Ulrych & Adamovič 2004) are rarely accompanied by independent kaersutitic hornblende xenocrysts.

Clinopyroxenite forms rare layers in lherzolite xenoliths and scarce clinopyroxenite discrete nodules in lavas of the Kozákov volcano (Vokurka & Povondra 1983; Medaris et al. 1997). Clinopyroxenite xenoliths of similar composition were described by Mihaljevič (1993) from the basanite flow in the central part of the České středohoří Mts, Ulrych et al. (2000) from the Osečná Complex in the lateral block of the Ohře Rift in N Bohemia, and by Ulrych et al. (2005) from the Loučná–Oberwiesenthal Volcanic Centre in a similar structural position in the Krušné hory Mts, (Fig. 1).

The aim of the paper is to contribute to the estimation of P-T-f_{O_2} conditions and to decipher the geochemical character of the upper mantle beneath the Kozákov volcano based on the study of the major, minor and trace element chemistry of xenoliths of different lithologies, textural types and their mineral phases.

Geological setting

The Kozákov volcano (743 m a.s.l., see geological sketch in Figs. 1 and 2) is situated in NE Bohemia on an arm of the Lužice (Lusatian) fault bordering the Labe Tectono-volcanic Zone, a prominent Cenozoic structure of the Bohemian Massif. Lava flows of the Kozákov volcano have been exposed in many quarries. Three lava

flows of the Early Pliocene ages (3.95 Ma for the uppermost, 4.14 Ma for the lowermost flows in the Smrčí–Proseč area (cf. Šibrava & Havlíček 1980) were recognized (cf. Fediuk 1968). Wilson et al. (1994) presented the age of 4.25 Ma for the lowermost flow from Slap quarry. Nevertheless, ages of 6.39 Ma and 6.60 Ma for the lowermost flows were published by Bellon & Kopecký (1977) and Šibrava & Havlíček (1980), respectively. The lowermost lava flow can be divided into an upper, thicker part with thin columnar entablature, and a basal false colonnade with thick columns (Fediuk in Ulrych et al. Eds. 1991). Radiometric ages of the lava flow correspond to its geological position (overlying old terrace sediments of the Jizera River) and stratigraphical position (palynological evidence for Middle Miocene age — Konzalová 1973).

Methods of study

Although ultramafic mantle xenoliths are present in all lava flows of the Kozákov volcano, they can be collected from the lowermost flow of the Smrčí–Proseč–Slap area only. Previously collected samples from the locality of Pelechov were used for a comparison, see Fig. 2. Quarries in other areas of the Kozákov volcano with the uppermost lava flows have been closed many years ago. The xenoliths were studied macroscopically in the quarries in much detail, and microscopically in thin sections.

Quantitative (magnetic and heavy liquid) separation of mineral fractions of olivine, orthopyroxene, clinopyroxene and spinel was applied to the study of two ellipsoidal lherzolite xenoliths from two localities: Smrčí — 1.727 kg, and Slap — 4.175 kg. Separation was performed on 1100 g of crushed original rock from Smrčí and 1500 g from Slap, using the most frequent size fractions of 0.125–0.250 mm. Final concentrates were tested for purity (98–99 %) using an optical method.

The composition of mineral phases of ultramafic xenoliths was determined using a CamScan 4–Link-eXL electron microprobe (Analyst R. Rybka, Czech Geological Survey, Praha) with an acceleration voltage of 15 kV, beam current of 20 nA, beam size about 3–5 mm, counting time 20 s for peaks and 5 s for background, both natural and synthetic standards and the ZAF reduction program.

Major element concentrations in the host rock, ultramafic xenoliths and their mineral fractions were determined using wet chemical methods (Analyst P. Povondra, Charles University, Praha). Analyses of the international reference whole-rock standards (GM, TB, BN) and duplicate analyses of the samples suggest total errors of ±5 % (1 s.d.).

Trace element concentrations were determined by instrumental neutron activation analysis (INAA). Powdered samples 50–90 mg in weight were sealed in polyethylene foils and irradiated for 4 hours in a nuclear reactor LWR-15 of the Institute of Nuclear Research at Řež. The neutron flux rate was $8.5\times10^{13}\,cm^{-2}\cdot s^{-1}$. The irradiated

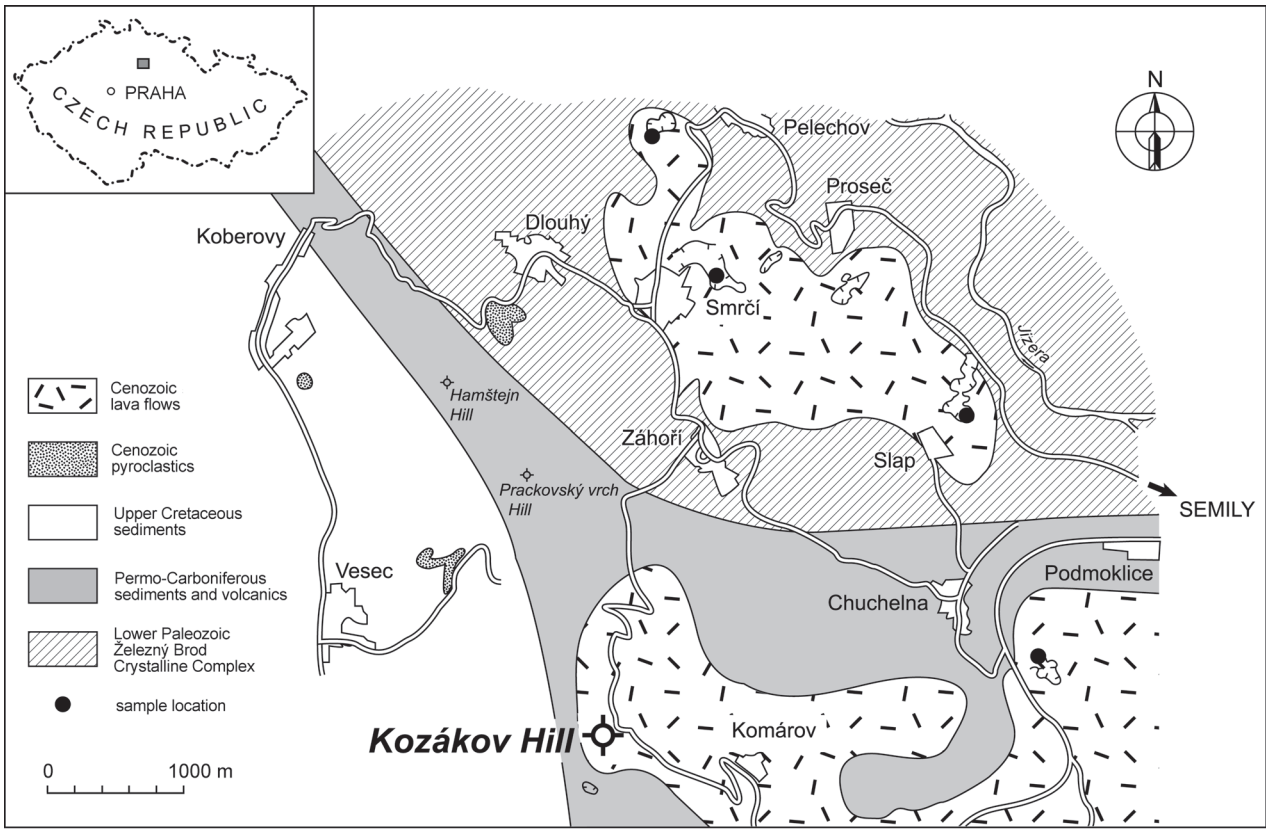

Fig. 2. A sketch of the geological setting of the Kozákov volcano lava flows (modified after Kopecký 1968).

samples were measured after three days and four months. The gamma-ray spectrometric system, equipped with a HPGe-detector, was operated with the following parameters: efficiency 22 % and resolution FWHM 1.8 keV for photons 1332.5 keV of ^{60}Co. The counting time was 1.5 hours in the first run and 24 hours in the second one. The precision (1 s.d.) is better than ±10 % for the REE and ±5 to 10 % for other trace elements. The accuracy of the data was checked against international rock standards. It is better than 10 % for the REE and 5 % for the other trace elements.

A quadrupole-based inductively coupled plasma mass spectrometry (ICP-MS) (VG Elemental PQ3, UK) was used for determination of REE and other trace element contents (Analyst L. Strnad, Charles University, Praha). Parameter Values: Rf power (W) — 1420, gas flows (l/min Ar 5.0) — 13.5, 1.3, 0.72, acquisition time of 3.50 s, nebulizer of Meinhard type, acquisition mode — peak jump, points per peak — 3, dwell time — 10.24, replicates — 3, detector mode — pulse, internal standards — ^{45}Sc, ^{115}In, ^{185}Re. The precision (1σ) for incompatible elements was better than ±5 %. Accuracy was checked using above mentioned international reference rock standards. Detection limits are in μg/l (ppb).

Characteristics of the xenoliths

Ultramafic xenoliths constitute about 99 % of all xenoliths in basaltic flows of the Kozákov volcano (Fediuk 1968). Harzburgites and lherzolites (about 96 %) prevail over dunites (3 %) and ortho- and clinopyroxenites (1 %). Modal compositions calculated from bulk-rock compositions and mineral compositions plot the ultramafic xenoliths from the Kozákov volcano to the lherzolite field, less frequently to the harzburgite, dunite and wehrlite fields (Fig. 3).

On the basis of field observations, the proportion of ellipsoidal xenoliths 1 to 70 cm in size was estimated at 2 vol. % of the total rock volume (Fediuk 1968). The total volume of xenolithic material is likely approaching 10 vol. % if discrete nodules and xenocrysts are included. About 50 % of all xenoliths were 1–2 cm in size, xenoliths larger than 5 cm represent 10 % (Fediuk 1968). In many cases, however, the original size of the xenoliths was originally larger than given above as the xenoliths are angular fragments originated during magma transport and/or solidification of the host magma.

The contact of the xenoliths with the host rock is mostly sharp. The reaction rim at the contact of the xenolith with the host rock is 0.3 to 0.8 mm wide only. A broader clouded amphibolized zone was observed only around orthopyroxene at contact with the host rock. Rare elongation of olivines and pyroxenes in xenoliths (?) was observed, partly highlighted by spinel arrangement to elongated clusters. Microscopic study of the xenoliths confirmed two distinct types of textures: a dominant medium- to coarse-grained protogranular and minor medium-grained equigranular type and rare porphyroclastic types (Table 1) (sensu Mercier & Nicolas 1975).

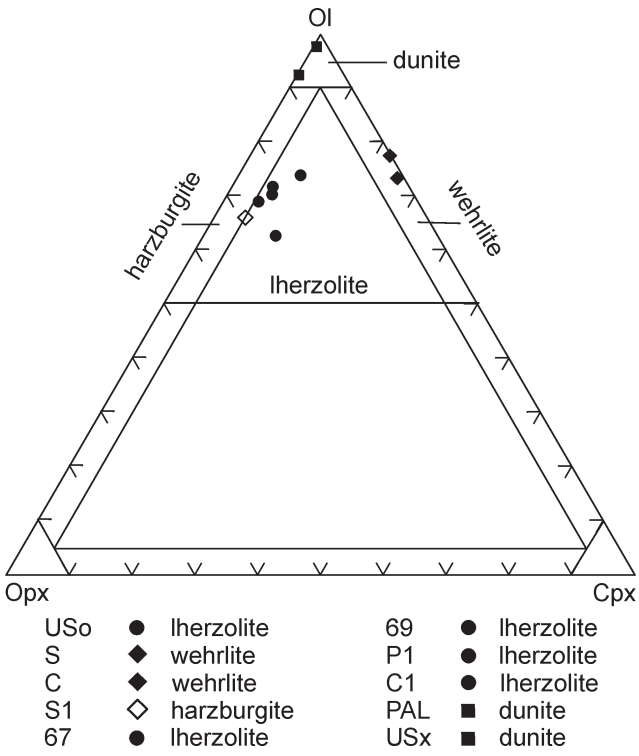

Fig. 3. Classification diagram for peridotites (Streckeisen 1979). Modal abundances calculated by least square fitting of measured mineral composition to the bulk-rock analyses. Where the respective minerals were not analysed, average data from literature on compositions of phases from ultramafic xenoliths were used. SiO_2, TiO_2, Al_2O_3, Cr_2O_3, FeO_t, MnO, MgO, CaO, and Na_2O contents were involved in multilinear regression, Σr^2 was better than 0.98 for all samples.

Mineral chemistry

Mineral chemistry was studied using four methods: wet analyses of pure mineral fractions (99–100 %) used for the trace element study, ICP-MS, INAA (Table 2), and microprobe analyses in thin sections (Tables 3 and 4).

Olivine reveals generally high forsterite contents ($Fo_{89.4–91.8}$) compatible with the composition of upper mantle olivines. The variation of Fo content in olivines within singular samples is small. A comparison of the chemical composition of olivine between samples indicates certain correlations: the lowest Fo values were encountered in lherzolite S4x with porphyroclastic texture (~$Fo_{89.2}$), low to intermediate values were found in protogranular lherzolites ($Fo_{89.4–90.6}$), and the highest values in harzburgites ($Fo_{91.2–91.8}$). No significant differences were found either between cores and rims or between small and large crystals.

Orthopyroxene and clinopyroxene are both highly magnesian, showing narrow ranges of *Mg*-number [(Mg/(Mg+Fe)*100] of 88.4–93.7 and 89.4–91.6, respectively. Orthopyroxenes from harzburgites yield higher values (91.0–93.7), whereas lherzolites yield lower values (88.3–91.4). In contrast, *Mg*-numbers of clinopyroxenes in harzburgites (89.4–90.6) and lherzolites (89.5–91.5)

Table 1: List of samples of ultramafic xenoliths and their host rocks from the Kozákov volcano.

Sample No.	Rock/texture	Locality	Reference
67	lherzolite/protogranular	Smrčí quarry	
69	medium-grained lherzolite/protogranular	Smrčí quarry	
C	wehrlite	Chuchelna quarry	Vokurka (1979)
C1	lherzolite/protogranular	Chuchelna quarry	Jakeš & Vokurka (1987)
C1v	lherzolite/equigranular	Chuchelna quarry	Vokurka (1979)
C2v	harzburgite/protogranular	Chuchelna quarry	Vokurka (1979)
F1	pyroxenite/protogranular?	Smrčí quarry	Farský (1876)
F2	pyroxenite/protogranular?	Smrčí quarry	Farský (1876)
P1	medium- to coarse-grained lherzolite/protogranular	Pelechov quarry	Schovánek (1977)
P1x	medium- to coarse-granined lherzolite/protogranular	Pelechov quarry	Schovánek (1977)
P4x	medium- to coarse-granined harzburgite/protogranular	Pelechov quarry	Schovánek (1977)
PAL	dunite	Smrčí quarry	
S	wehrlite	Smrčí quarry	Vokurka (1979)
S1	fine- to medium-grained harzburgite/protogranular to equigranular	Smrčí quarry	Schovánek (1977)
S1v	harzburgite	Smrčí quarry	Vokurka (1979)
S1x	lherzolite	Smrčí quarry	Schovánek (1977)
S1v	harzburgite	Smrčí quarry	Vokurka (1979)
S2v	lherzolite	Smrčí quarry	Vokurka (1979)
S4x	lherzolite/porphyroclastic	Smrčí quarry	Schovánek (1977)
USo	medium- to coarse-grained lherzolite/protogranular	Slap quarry	
USx	dunite	Smrčí quarry	
SM	basanite	Smrčí quarry	Wilson et al. (1994)
SL	basanite	Slap quarry	

Table 2: Trace element analyses (in ppm) of minerals from protogranular lherzolite and host basanite from Slap, Kozákov volcano. Modal composition according to separated mineral phases: xenolith 67 (ICP-MS) — olivine 58 %, clinopyroxene 12 %, orthopyroxene 25 %, spinel 5 % and xenolith USo (INAA) — olivine 56 %, clinopyroxene 15 %, orthopyroxene 24 %, spinel 5 %. SM and SL (INAA) — bulk-rock analyses, n.d. — not determined.

Sample	67	67	67	67	USo	USo	USo	USo	SM	SL
Min./Rock	olivine	orthopyroxene	clinopyroxene	spinel	olivine	orthopyroxene	clinopyroxene	spinel	basanite	basanite
Sc	n.d.	n.d.	n.d.	n.d.	2.5	22.7	43.9	1.9	23.0	18.0
V	12.2	59.0	116.0	75.6	2.5	77	128	480	199	168
Cr	90	6 492	8 836	n.d	123	3 255	4 354	122 300	461	450
Co	94	45	31	41	136	57	39	241	55	53
Ni	3 832	698	495	464	2 782	786	558	2 661	436	421
Zn	n.d.	n.d.	n.d.	n.d.	43	37	35	774	94	101
Cu	1.9	3.5	5.5	16.8	n.d.	n.d.	n.d.	n.d.	n.d.	n.d.
Zr	0.58	0.79	0.59	1.00	n.d.	n.d.	n.d.	n.d.	n.d.	n.d.
Y	0.06	0.47	3.19	0.11	n.d.	n.d.	n.d.	n.d.	n.d.	n.d.
Nb	0.19	0.36	1.27	0.32	n.d.	n.d.	n.d.	n.d.	n.d.	n.d.
Rb	0.08	0.14	0.15	0.29	<0.2	<0.2	<0.2	<0.3	67	66
Sr	0.2	1.2	8.5	1.91	<260	<270	<270	<570	928	939
Cs	<0.010	<0.010	<0.010	<0.025	<0.01	<0.02	0.16	0.089	n.d.	n.d.
Ba	0.52	1.6	2.1	17.6	<10	<30	<40	<24	652	677
La	0.06	0.68	6.93	0.10	0.1	0.7	9.7	0.7	67.5	64.9
Ce	1.32	0.61	4.38	0.97	1.9	1.6	22.5	2.5	127.2	122.9
Pr	0.008	0.028	0.15	0.013	n.d.	n.d.	n.d.	n.d.	n.d.	n.d.
Nd	0.034	0.076	0.22	0.037	n.d.	n.d.	n.d.	n.d.	n.d.	n.d.
Sm	<0.01	<0.01	0.042	<0.025	0.008	0.028	1.3	0.009	8.42	8.31
Eu	<0.005	0.007	0.026	<0.01	0.0026	0.04	0.37	0.008	2.48	2.43
Gd	<0.01	0.024	0.148	<0.025	<0.1	<0.3	<1.0	<0.3	6.87	6.88
Tb	<0.005	<0.005	0.042	<0.01	<0.003	<0.01	<0.2	<0.01	1.22	1.14
Dy	<0.01	0.055	0.406	<0.025	n.d.	n.d.	n.d.	n.d.	n.d.	n.d.
Ho	<0.005	0.021	0.112	<0.01	<0.002	0.061	0.15	<0.002	0.95	0.93
Er	<0.01	0.065	0.410	<0.025	n.d.	n.d.	n.d.	n.d.	n.d.	n.d.
Tm	<0.005	0.013	0.066	<0.01	n.d.	n.d.	n.d.	n.d.	n.d.	n.d.
Yb	<0.01	0.105	0.464	<0.025	0.007	0.55	0.76	0.007	2.05	2.04
Lu	<0.005	0.017	0.074	<0.01	0.003	0.11	0.105	0.002	0.32	0.30
Hf	<0.05	<0.05	<0.05	<0.10	<0.04	<0.2	<0.2	<0.5	6.21	5.86
Ta	0.13	0.08	0.09	0.065	n.d.	n.d.	n.d.	n.d.	n.d.	n.d.
Th	0.12	0.15	1.46	0.066	0.2	0.31	1.7	<0.3	8.7	8.9
U	0.022	0.04	0.29	0.042	<0.8	<0.8	<0.9	<1.8	2.6	3.1

Table 3: Representative analyses and number of ions per formula unit calculated to 4 oxygens (olivine — ol) and 3 cations (spinel — sp) of ultramafic xenoliths from the Kozákov volcano. * — wet analyses, all other microprobe analyses, n.a. — not analysed.

Sample	**67***	**USo***	**F1***	**F2***	**S1v**	**S2v**	**C1v**	**C2v**	**S1x**	**S4x**	**S4x**	**P1x**	**P4x**	**67***	**S4x**	**S4x**	**S1x**	**P1x**	**P4x**	**P4x**
Mineral	ol	ol	ol	ol	ol	ol	ol	ol	ol	ol	ol	ol	ol	sp	sp	sp	sp	sp	sp	sp
SiO_2	41.14	40.48	41.15	41.22	40.48	40.61	40.80	40.80	40.51	39.48	41.39	40.41	41.14	1.83	1.32	1.47	1.15	0.88	0.64	0.56
TiO_2	0.01	n.a.	n.a.	n.a.	n.a.	0.01	0.00	0.02	0.03	n.a.	0.04	n.a.	0.04	0.32	n.a.	n.a.	n.a.	0.04	0.11	0.10
Al_2O_3	0.67	0.18	0.15	0.15	0.46	0.44	0.54	0.46	0.26	0.31	0.32	0.18	0.16	36.88	41.97	16.96	41.84	45.59	32.78	35.30
FeO	8.71	10.21	9.15	9.10	7.97	7.97	7.82	8.05	8.21	10.38	8.40	9.17	8.51	14.95	12.64	36.86	10.84	13.26	16.59	15.53
MnO	0.07	0.14	0.15	0.18	0.22	0.13	0.22	0.13	0.11	0.17	0.14	0.10	0.14	0.41	n.a.	n.a.	n.a.	1.13	0.20	0.16
MgO	48.21	48.09	49.51	49.42	49.07	49.55	49.22	49.72	48.58	48.29	49.82	49.84	49.28	18.90	21.41	13.68	22.60	18.86	13.86	14.62
CaO	0.09	0.10	n.a.	n.a.	0.20	0.22	0.23	0.24	0.41	0.14	0.41	0.07	0.08	0.21	n.a.	0.22	0.16	0.07	0.15	0.02
Cr_2O_3	n.a.	n.a.	n.a.	n.a.	n.a.	n.a.	n.a.	n.a.	n.a.	n.a.	n.a.	n.a.	n.a.	24.18	21.84	29.56	22.26	20.68	34.09	31.72
NiO	0.57	0.35	0.20	0.29	0.39	0.35	0.35	0.33	0.23	n.a.	0.23	n.a.	n.a.	0.13	n.a.	n.a.	n.a.	n.a.	n.a.	n.a.
Total	99.47	99.55	100.31	100.36	98.79	99.28	99.18	99.75	98.34	98.77	100.75	99.77	99.35	97.81	99.18	98.75	98.85	100.51	98.42	98.01
Si	1.008	0.999	1.002	1.003	0.998	0.996	1.000	0.996	1.003	0.984	1.001	0.990	1.007	0.052	0.036	0.046	0.031	0.024	0.019	0.016
Ti	0.000	0.000	0.000	0.000	0.000	0.000	0.000	0.000	0.001	0.000	0.001	0.000	0.001	0.007	0.000	0.000	0.000	0.001	0.002	0.002
Al	0.019	0.005	0.004	0.004	0.013	0.013	0.016	0.013	0.008	0.009	0.009	0.005	0.005	1.230	1.342	0.623	1.333	1.449	1.146	1.221
Fe	0.178	0.211	0.186	0.185	0.164	0.163	0.160	0.164	0.170	0.216	0.170	0.188	0.174	0.354	0.287	0.960	0.245	0.299	0.411	0.381
Mn	0.001	0.003	0.003	0.004	0.005	0.003	0.005	0.003	0.002	0.004	0.003	0.002	0.003	0.010	0.000	0.000	0.000	0.026	0.005	0.004
Mg	1.761	1.770	1.797	1.793	1.803	1.811	1.799	1.809	1.793	1.795	1.796	1.820	1.798	0.798	0.866	0.635	0.911	0.758	0.613	0.639
Ca	0.002	0.003	0.000	0.000	0.005	0.006	0.006	0.006	0.011	0.004	0.011	0.002	0.002	0.006	0.000	0.007	0.005	0.002	0.005	0.001
Na	0.000	0.000	0.000	0.000	0.000	0.000	0.000	0.000	0.000	0.000	0.000	0.000	0.000	0.000	0.000	0.000	0.000	0.000	0.000	0.000
K	0.000	0.000	0.000	0.000	0.000	0.000	0.000	0.000	0.000	0.000	0.000	0.000	0.000	0.000	0.000	0.000	0.000	0.000	0.000	0.000
Cr	0.000	0.000	0.000	0.000	0.000	0.000	0.000	0.000	0.000	0.000	0.000	0.000	0.000	0.541	0.469	0.728	0.476	0.441	0.799	0.736
Ni	0.007	0.004	0.003	0.004	0.005	0.004	0.004	0.004	0.003	0.000	0.003	0.000	0.000	0.002	0.000	0.000	0.000	0.000	0.000	0.000
Cations	2.978	2.996	2.995	2.993	2.993	2.996	2.990	2.995	2.991	3.011	2.993	3.007	2.990	3.000	3.000	3.000	3.000	3.000	3.000	3.000
Fe^{3+}														0.184	0.134	0.357	0.085	0.214	0.378	0.356
Fe^{2+}														0.170	0.153	0.603	0.160	0.085	0.034	0.025
Cr/(Cr+Al)*100														30.5	25.9	53.9	26.3	23.3	41.1	37.6
Mg/(Mg+Fe_t)*100	90.8	89.4	90.6	90.6	91.6	91.7	91.8	91.7	91.3	89.2	91.4	90.6	91.2							

Table 4: Representative analyses of orthopyroxene (opx) and clinopyroxene (cpx) and number of ions per formula unit calculated to 6 oxygens of ultramafic xenoliths from the Kozákov volcano. * — wet analyses, all other microprobe analyses, n.a. — not analysed.

Sample	**67***	**USo***	**F1***	**F2***	**C1v**	**C2v**	**S1v**	**S2v**	**S1x**	**S4x**	**P1x**	**P4x**	**67***	**USo***	**F1***	**F2***	**C1v**	**C2v**	**S1v**	**S2v**	**S4x**	**P1x**
Mineral	opx	opx	opx	opx	opx	opx	opx	opx	opx	opx	opx	opx	cpx	cpx	cpx	cpx	cpx	cpx	cpx	cpx	cpx	cpx
SiO_2	54.00	53.90	53.29	54.01	55.21	53.84	52.70	54.10	56.61	53.72	54.29	56.08	52.07	50.66	53.44	52.92	51.27	50.51	51.13	51.81	53.13	53.18
TiO_2	0.01	0.01	n.a.	n.a.	0.10	0.08	0.07	0.08	0.11	0.03	0.03	0.05	0.08	0.02	n.a.	n.a.	0.25	0.25	n.a.	0.24	0.11	0.07
Al_2O_3	3.81	4.62	2.77	2.52	4.59	4.19	5.94	3.51	2.52	4.66	3.90	2.40	5.23	5.12	3.74	3.54	5.78	5.25	5.42	4.67	5.66	4.84
FeO	7.70	6.26	15.43	15.27	5.00	5.28	3.93	5.09	5.92	5.48	5.69	5.88	3.16	3.95	4.70	4.75	3.15	3.14	3.57	3.35	2.83	2.75
MnO	0.06	0.14	n.a.	n.a.	0.19	0.14	0.11	0.14	0.17	0.09	0.09	0.11	0.04	0.09	0.31	0.30	0.17	0.09	0.20	0.09	0.08	0.08
MgO	32.74	32.85	27.01	27.75	31.85	33.02	33.00	33.04	33.37	32.45	33.74	34.13	17.26	18.93	16.99	17.43	16.26	17.07	16.89	17.15	17.02	16.48
CaO	0.13	1.45	1.19	0.74	1.52	2.04	2.27	2.48	0.80	1.10	0.80	0.43	19.22	18.65	19.90	19.99	21.28	21.71	22.01	21.81	19.26	20.88
Na_2O	0.17	0.05	n.a.	n.a.	n.a.	n.a.	n.a.	n.a.	0.03	0.10	0.07	0.02	1.28	0.69	n.a.	n.a.	n.a.	n.a.	n.a.	n.a.	1.05	0.87
K_2O	0.07	0.01	n.a.	n.a.	n.a.	n.a.	n.a.	n.a.	n.a.	n.a.	n.a.	n.a.	0.07	0.18	n.a.	n.a.	n.a.	n.a.	n.a.	n.a.	n.a.	n.a.
Cr_2O_3	0.48	0.73	n.a.	n.a.	0.52	0.53	0.99	0.57	0.39	0.67	0.53	0.39	1.17	1.43	0.75	0.74	0.89	0.92	0.76	1.19	1.07	0.89
Total	99.18	100.02	99.69	100.29	98.98	99.12	99.01	99.01	99.92	98.30	99.14	99.49	99.59	99.72	99.83	99.67	99.05	98.94	99.98	100.31	100.21	100.04
Si	1.895	1.872	1.927	1.936	1.918	1.881	1.836	1.893	1.952	1.887	1.892	1.942	1.891	1.848	1.941	1.929	1.876	1.857	1.863	1.879	1.907	1.920
Ti	0.000	0.000	0.000	0.000	0.003	0.002	0.002	0.002	0.003	0.001	0.001	0.001	0.002	0.001	0.000	0.000	0.007	0.007	0.000	0.007	0.003	0.002
Al	0.158	0.189	0.118	0.106	0.188	0.172	0.244	0.145	0.102	0.193	0.160	0.098	0.224	0.220	0.160	0.152	0.249	0.228	0.233	0.200	0.239	0.206
Fe	0.226	0.182	0.467	0.458	0.145	0.154	0.115	0.149	0.171	0.161	0.166	0.170	0.096	0.121	0.143	0.145	0.096	0.097	0.109	0.102	0.085	0.083
Mn	0.002	0.004	0.000	0.000	0.006	0.004	0.003	0.004	0.005	0.003	0.003	0.003	0.001	0.003	0.010	0.009	0.005	0.003	0.006	0.003	0.002	0.002
Mg	1.713	1.701	1.456	1.483	1.649	1.719	1.714	1.723	1.715	1.699	1.753	1.762	0.935	1.030	0.920	0.947	0.887	0.936	0.918	0.927	0.911	0.887
Ca	0.005	0.054	0.046	0.028	0.057	0.076	0.085	0.093	0.030	0.041	0.030	0.016	0.748	0.729	0.774	0.781	0.834	0.855	0.859	0.847	0.741	0.808
Na	0.012	0.003	0.000	0.000	0.000	0.000	0.000	0.000	0.002	0.007	0.005	0.001	0.090	0.049	0.000	0.000	0.000	0.000	0.000	0.000	0.073	0.061
K	0.003	0.001	0.000	0.000	0.000	0.000	0.000	0.000	0.000	0.000	0.000	0.000	0.003	0.008	0.000	0.000	0.000	0.000	0.000	0.000	0.000	0.000
Cr	0.013	0.020	0.000	0.000	0.014	0.015	0.027	0.016	0.011	0.019	0.015	0.011	0.034	0.041	0.022	0.021	0.026	0.027	0.022	0.034	0.030	0.025
Ni	0.000	0.000	0.000	0.000	0.000	0.000	0.000	0.000	0.000	0.000	0.000	0.000	0.000	0.000	0.000	0.000	0.000	0.000	0.000	0.000	0.000	0.000
Cations	4.027	4.026	4.014	4.011	3.979	4.024	4.026	4.025	3.990	4.010	4.023	4.004	4.025	4.049	3.969	3.984	3.980	4.009	4.010	3.998	3.992	3.993
Fe^{3+}	0.053	0.050	0.028	0.022	0.000	0.047	0.052	0.049	0.000	0.020	0.045	0.007	0.049	0.097	0.000	0.000	0.000	0.017	0.019	0.000	0.000	0.000
Fe^{2+}	0.849	0.854	0.813	0.810	0.814	0.854	0.863	0.857	0.817	0.836	0.850	0.826	0.889	0.920	0.840	0.848	0.852	0.874	0.873	0.864	0.855	0.858
$Mg/(Mg+Fe_t)*100$	88.3	90.3	75.7	76.4	91.9	91.8	93.7	92.0	90.9	91.3	91.4	91.2	90.7	89.5	86.6	86.7	90.2	90.6	89.4	90.1	91.5	91.4
Wo	0.3	2.8	2.3	1.4	3.1	3.9	4.4	4.7	1.5	2.2	1.5	0.8	42.1	38.8	42.2	41.7	45.9	45.3	45.6	45.2	42.7	45.4
En	88.1	87.8	74.0	75.3	89.1	88.2	89.6	87.7	89.5	89.4	90.0	90.4	52.5	54.8	50.1	50.6	48.8	49.6	48.7	49.4	52.5	49.9
Fs	11.6	9.4	23.7	23.2	7.8	7.9	6.0	7.6	8.9	8.5	8.5	8.7	5.4	6.4	7.8	7.7	5.3	5.1	5.8	5.4	4.9	4.7

overlap. The lowest *Mg*-number for orthopyroxene was recorded in protogranular herzolite USo, in agreement with its fertile character reflected in the incompatible element contents. The positive trend of calcium content expressed as the number of Ca (p.f.u.) in orthopyroxene and clinopyroxene in Fig. 4 points to the coexistence relations of both pyroxenes. Clinopyroxenes from lherzolites USo and S4x are poor in number of Ca (p.f.u.) probably due to their incomplete re-equilibration. Better positive correlation was found in Al_2O_3 wt. % contents between the two pyroxenes (Fig. 5), supporting pyroxene coexistence.

Spinels are typically chromium-rich, with Cr_2O_3 contents varying between 21.8 and 34.1 wt. %. The ratio of

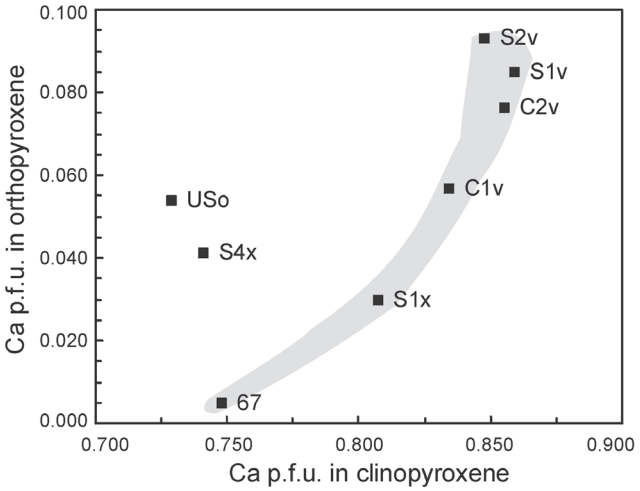

Fig. 4. Correlation between the number of Ca (p.f.u.) in clinopyroxene and orthopyroxene. A positive correlation was achieved except for samples USo and S4x.

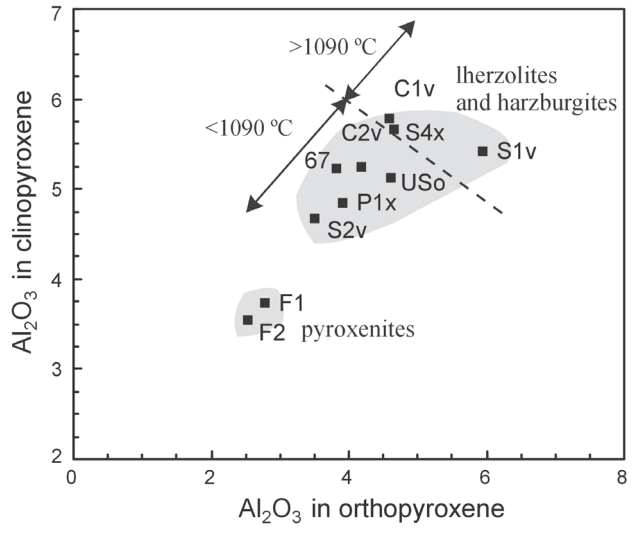

Fig. 5. Correlation between Al_2O_3 contents (wt. %) in coexisting ortho- and clinopyroxenes. Temperature data are listed in Table 5. The temperature of 1090 °C delimits the upper protogranular and the underlying equigranular mantle layer defined by Medaris et al. (1999).

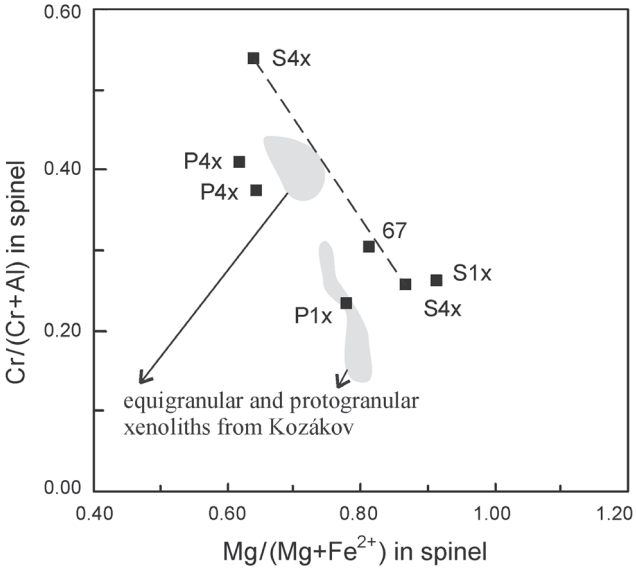

Fig. 6. Compositional variations in spinel in terms of Cr/(Cr+Al) vs. Mg/(Mg+Fe^{2+}) ratios. Shaded areas denote xenoliths from the Kozákov volcano after Medaris et al. (1999). The dashed line connects two types of spinel with remarkably different Cr/(Cr+Al) ratios in porphyroclastic lherzolite S4x.

Cr/(Cr+Al+Fe^{3+})*100 in protogranular lherzolites (S1x, P1x) is lower (22.3–27.9) than in harzburgites (37.1–40.4). Spinels from porphyroclastic xenolith S4x are very heterogeneous (23.9–37.3), suggesting a non-equilibrium origin of the sample. Unusual spinel from progranular lherzolite USo with 17.9 wt. % Cr_2O_3 and extremely high Al_2O_3 content (68.0) belongs to the Al-spinel group.

Variations in spinel composition are presented in Fig. 6. Protogranular and equigranular xenoliths recognized by Medaris et al. (1999), Christensen et al. (2001), and displayed as fields in Fig. 6, show a narrow scatter of data compared to the studied xenoliths. Fine-grained harzburgite P4x plots close to the equigranular lherzolite field. Spinels of other lherzolites plot near the protogranular lherzolite field. Spinel in porphyroclastic lherzolite S4x with high *Cr*-number approaches spinels from the equigranular field in its chemical composition, and the other spinels approach those from the protogranular field. The two types of spinel from protogranular lherzolite S4x connected with a dashed line show large differences in the Cr/(Cr+Al) ratio.

Bulk-rock analyses of major elements

Chemical composition of the studied lherzolite xenoliths (see Table 5) shows systematic variations if the elements are plotted against MgO, which is a sensitive indicator of the degree of depletion. Basalt-compatible oxides SiO_2, CaO, Al_2O_3, TiO_2 correlate negatively with MgO, as was observed in many xenoliths worldwide (e.g. Downes 2001 from the Central European Volcanic Province; Luhr & Aranda-Gómez 1997; Xu et al. 1998;

Table 5: Chemical analyses (wt. %) of peridotite xenoliths and host basanite from the Kozákov volcano: *Mg*-number — Mg/(Mg + Fe$_t$)*100, n.d. — not determined, n.a. — not analysed.

											host basalts	
Rock	**lherzolite**	**lherzolite**	**wehrlite**	**lherzolite**	**lherzolite**	**dunite**	**wehrlite**	**harzburgite**	**lherzolite**	**dunite**	**basanite**	**basanite**
Sample	67	69	C	C1	P1	PAL	S	S1	USo	USx	SM	SL
SiO_2	43.08	43.84	41.99	43.47	43.77	41.29	43.16	44.78	43.95	40.63	43.10	43.59
TiO_2	0.03	0.07	0.07	0.07	0.02	0.01	0.06	0.06	0.04	0.01	2.05	2.12
Al_2O_3	2.99	1.28	1.82	1.89	2.18	0.67	1.70	1.76	3.18	0.09	11.87	11.85
Cr_2O_3	0.31	0.49	0.65	0.68	0.29	0.08	0.34	0.35	0.37	0.04	n.d.	n.d.
Fe_2O_3	1.11	1.12	1.14	1.18	0.75	1.84	0.80	0.83	1.27	2.91	11.86	3.98
FeO	7.50	7.44	6.84	7.10	7.08	7.66	7.39	7.67	7.92	7.59	n.d.	7.31
MnO	0.12	0.22	0.22	0.23	0.13	0.15	0.24	0.25	0.14	0.13	0.21	0.20
MgO	42.23	42.33	41.25	42.84	42.70	47.50	40.36	41.88	40.34	48.26	14.61	14.14
CaO	2.01	1.99	5.57	1.85	1.54	0.25	5.43	1.80	2.50	0.11	10.70	10.59
Na_2O	0.04	0.07	0.07	0.07	0.14	0.10	0.08	0.08	0.07	n.d.	3.20	3.01
K_2O	0.01	0.01	n.d.	n.d.	0.02	0.03	n.d.	n.d.	0.02	n.d.	0.97	1.02
NiO	0.25	0.26	0.24	n.d.	n.d.	0.29	0.24	n.d.	0.25	0.33	n.d.	n.d.
P_2O_5	n.d.	n.d.	n.d.	n.d.	n.d.	n.d.	n.d.	n.d.	n.d.	n.d.	0.76	0.80
H_2O^+	n.d.	0.44	0.34	n.d.	0.36	0.28	0.44	n.d.	n.d.	n.d.	0.32	1.00
H_2O^-	n.d.	0.16	0.15	n.d.	0.05	n.d.	0.12	n.d.	n.d.	n.d.	n.d.	0.19
LOI	n.d.	n.a.	n.a.	0.51	n.a.	n.a.	n.a.	0.68	n.d.	n.d.	n.a.	n.a.
Total	99.68	99.72	100.35	99.89	99.03	100.15	100.36	100.14	100.05	100.10	99.64	99.80
Mg-number	90.1	90.2	90.6	90.6	90.9	90.5	90.1	90.1	89.1	90.0		
Ca/Al	0.61	1.41	2.78	0.89	0.64	0.34	2.90	0.93	0.71	1.11		
CaO/Al_2O_3	0.67	1.56	3.06	0.98	0.71	0.37	3.19	1.02	0.79	1.22		

Parkinson & Pearce 1988). Linear correlations of Al_2O_3, NiO and CaO vs. MgO contents for the studied xenoliths clearly visible in Fig. 7 (data listed in Table 5) can be related to the depletion by multiple melt extraction from the mantle. Straight-line correlations between SiO_2, TiO_2 and Na_2O vs. MgO contents are not very significant. The source material for melting is supposed to be the primitive average mantle. None of the studied xenoliths is close to the average primitive mantle composition, suggesting that all samples represent residua depleted after partial melting. The most strongly depleted samples with the highest MgO content (olivine discrete xenoliths — PAL and USx) plot on the opposite side of the depletion trend having the lowest Al_2O_3, TiO_2, SiO_2 and CaO concentrations. Nickel content increases with the degree of depletion except for sample PAL, indicating supplemental processes modifying Ni content. Samples from Chuchelna (C) and Smrčí (S) are remarkably enriched in CaO, with contents even exceeding those of the primitive mantle, while SiO_2 is relatively low. Such high concentrations cannot be explained by variations in mineralogy, but rather correspond to the presence of calcite microveinlets also associated with alteration in subsolidus conditions.

Distribution of REE and other trace elements in the mafic xenoliths and their clinopyroxenes

Trace element data on four separated mineral phases from protogranular lherzolite 67 and USo are given in Table 2. Bulk-rock contents were calculated using modal abundances of four constituent mineral phases and their trace element contents. The bulk-rock Ni and Co contents (2114 and 108 ppm) are comparable with those in lherzolites from continental rift zones and those from oceanic within-plate settings summarized by Siena & Coltorti (1993). Scandium accumulates preferentially in clinopyroxene and olivine, whereas Ni and Co accumulate in olivine only.

The C1-normalized bulk-rock REE pattern is governed by the contribution of clinopyroxenes (McDonough et al. 1992a; Xu et al. 1998). The trace element analyses of the clinopyroxene and the host rock (Table 2) show a clear coherency of C1-normalized REE pattern, but with different abundances (Fig. 8).

The C1-normalized REE pattern of clinopyroxene from the Kozákov lherzolite USo presented in Fig. 8 shows relative LREE enrichment with $(La_N/Lu_N)_{cpx} = 9.6$. Both the bulk rock and clinopyroxene in protogranular lherzolite USo display a flat REE pattern from MREE to HREE, but with apparent LREE enrichment. Similar REE patterns of lherzolites from the Western and Central European Volcanic Provinces (Downes 2001), Wangqing, China (Xu et al. 1998), Zabargad, Red Sea (Piccardo et al. 1993), Mt Lessini and Antarctica (Siena & Coltorti 1993), Balaton Highland Volcanic Field, Hungary (Downes et al. 1992) document LREE enrichment in metasomatized lherzolites. The observed LREE-rich pattern is comparable with REE pattern in clinopyroxenes from equigranular xenoliths depleted in basaltic compositions (CaO < 2 wt. %), in which orthopyroxene prevails over clinopyroxene (Downes et al. 1992; Xu et al. 1998; Downes 2001). Protogranular lherzolite USo is LREE-enriched, with CaO content of ~2.5 wt. %, an average *Mg*-number of ~0.89, and a higher Al/Si ratio, which is conformable with lherzolites/harzburgites enrichment in incompatible elements.

C1-normalized REE pattern of protogranular lherzolite 67 is different. It has a U-shaped pattern similar to the

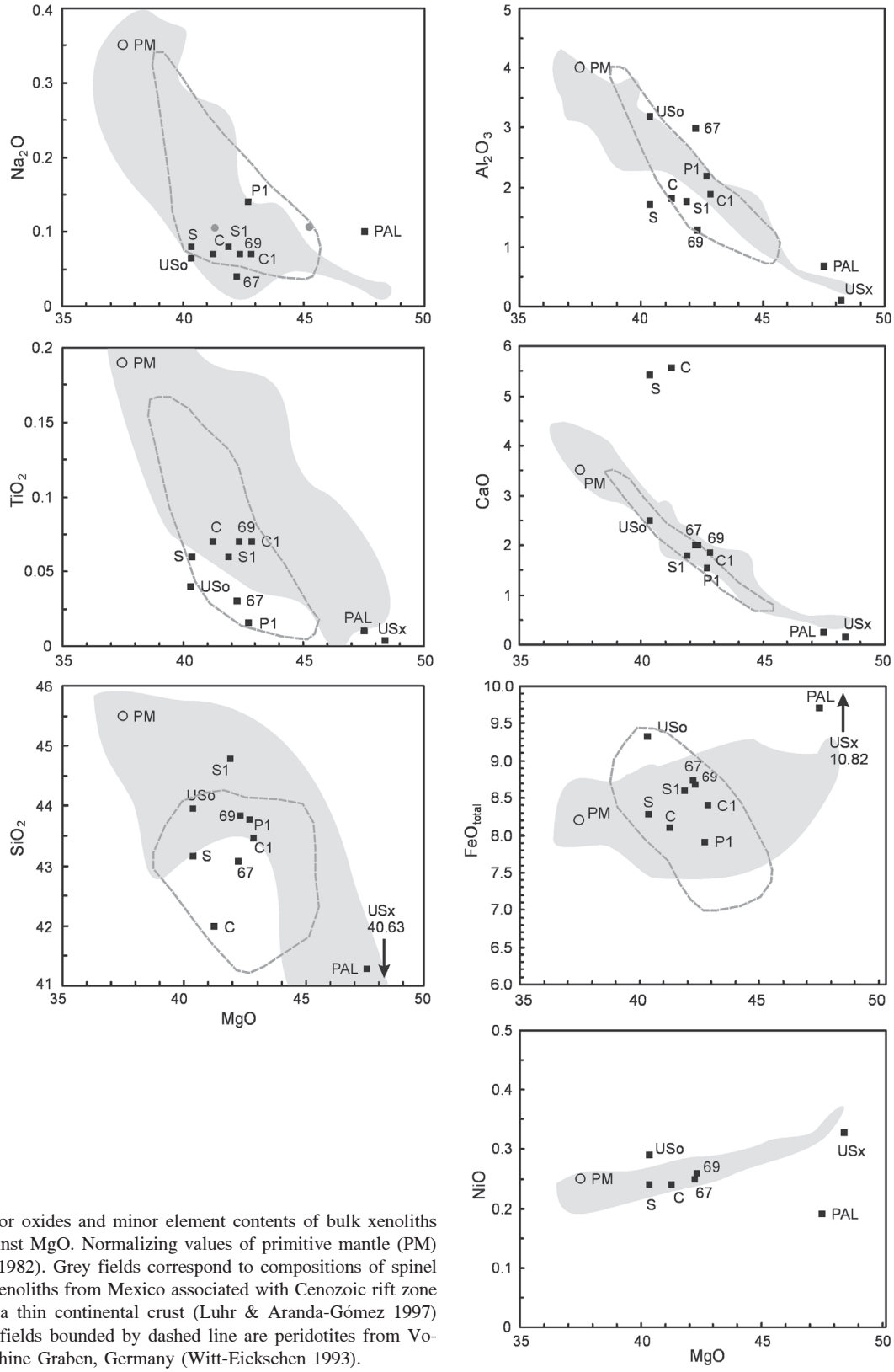

Fig. 7. Major oxides and minor element contents of bulk xenoliths plotted against MgO. Normalizing values of primitive mantle (PM) from Sun (1982). Grey fields correspond to compositions of spinel peridotite xenoliths from Mexico associated with Cenozoic rift zone located on a thin continental crust (Luhr & Aranda-Gómez 1997) and empty fields bounded by dashed line are peridotites from Vogelsberg, Rhine Graben, Germany (Witt-Eickschen 1993).

protogranular or in transitional between protogranular and equigranular xenoliths found in Eifel, Germany (Stosh et al. 1986), Massif Central, France (Downes & Dupuy 1987; Lenoir et al. 2000), Wangqing, China (Xu et al. 1998).

Upward LREE inflection and the U-shaped C1-normalized REE patterns, in the case of Kozákov lherzolites, suggests metasomatic processes modifying the original mantle composition.

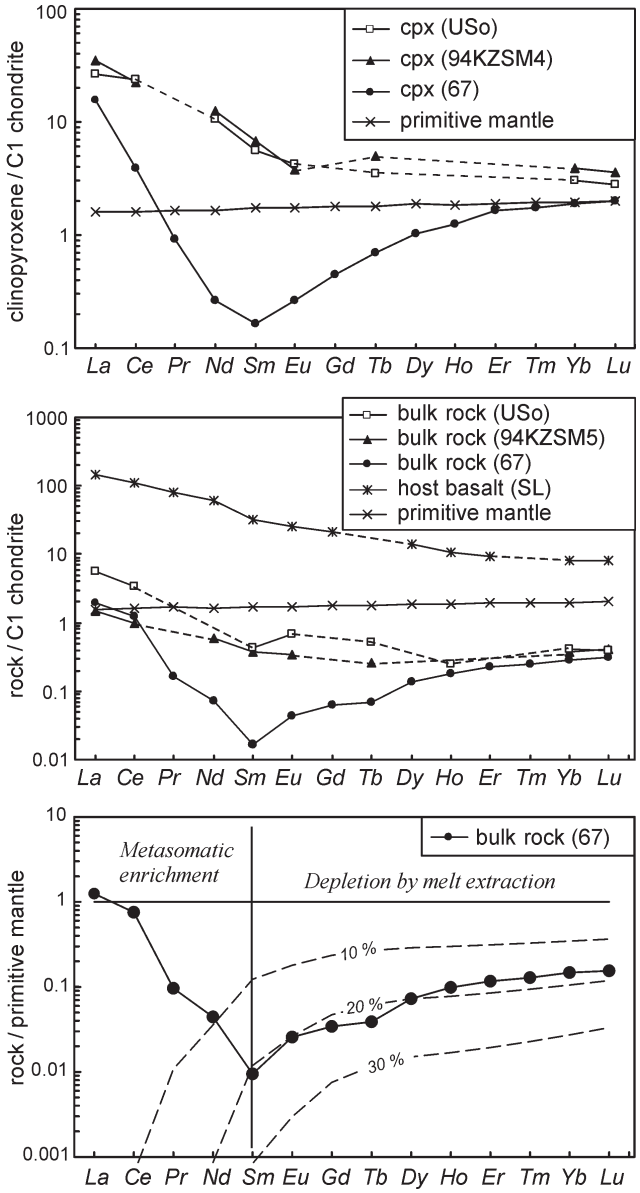

Fig. 8. C1-normalized REE patterns of lherzolites, clinopyroxenes, host basanite from the Kozákov volcano and of primitive mantle (McDonough et al. 1992b). Normalizing values of C1 chondrite from Taylor & McLennan (1985). Two types of pattern are clearly distinguishable: (1) LREE enriched, protogranular lherzolite USo and equigranular lherzolite 94KZSM4 from Smrčí (unpublished data of E. Jelínek) and (2) U-shape REE pattern in protogranular lherzolite 67. Dashed lines contour 10–30 % batch partial melting residuum of primitive mantle, partition coefficients taken from Ionov et al. (2002).

P-T-f$_{O_2}$ *conditions*

Spinel lherzolite assemblages do not allow reliable pressure calculations to be made. The only available barometer, based on Ca partitioning between olivine and clinopyroxene (Köhler & Brey 1990), yields a wide pressure range, almost independent on equilibration temperatures, with the *P-T* path being non-conformable with the geothermal gradient (Medaris et al. 1999; Konečný et al. 1999). The main reason for this is the different diffusion rate of Ca in both minerals, much higher in olivine than in clinopyroxene. During fast cooling of mantle xenoliths after a rapid ascent of the host magma, the Ca distribution in both minerals is inhomogeneous. Pressure calculations are then spurious. Errors may also be introduced by analytical methods. Measurement of low Ca concentrations in olivine calls for special care with microprobe calibration or the use of secondary ion mass spectrometry (SIMS) analyses. Instead of "absolute" pressure, a reasonable pressure range might be deduced from the position of spinel/garnet and spinel/plagioclase phase transition. The upper pressure limit is constrained by the Moho discontinuity. Spinel is stabilized by an increasing Cr content (O'Neill 1981; Webb &Wood 1986). Calculated pressures of the spinel/garnet phase boundary for spinels with *Cr*-number of 0.2–0.4 using the method of O'Neill (1981) range from 2.4 to 3.0 GPa. The present thickness of the crust beneath the Kozákov volcano is about 32 km (Čermák et al. 1991). Consequently, using an average density of 3.3 g·cm^{-3}, the xenoliths are collected from depths of ~32 km down to 74 km (the most aluminium-rich spinel) to 92 km (the most chromium-rich spinel).

The two-pyroxene thermometer (Brey & Köhler 1990) was used for the calculation of equilibrium temperatures. A constant pressure of 1.5 GPa was assumed. All calculated temperatures from 10 samples (Table 6) lie in a very narrow range, from 1052 to 1165 °C. The lowest temperatures were recorded in pyroxenites F1, F2. The porphyroclastic lherzolite xenolith S4x reveals the highest temperature, thereby confirming its complex origin. Temperatures do not seem to depend strictly on the type of the xenolith, whether compared with harzburgite or lherzolite.

Oxygen fugacity is a parameter characterizing the redox state of the xenoliths and consequently also of the upper mantle. Oxygen fugacity conditions depend on the content of ferric iron in spinel, being in equilibrium with oxygen exchange between spinel, olivine, orthopyroxene and clinopyroxene. One of the most accepted versions of oxygen fugacity calculation (Ballhaus et al. 1991) was used. The pressure of 1.5 GPa and the temperature 1100 °C (average temperature of our two-pyroxene thermometer calculations) were taken as the mean mantle conditions beneath the Kozákov area. The range of oxygen fugacity calculated for four samples clusters above the fayalite-magne-

Table 6: Two-pyroxene temperatures calculated after Köhler & Brey (1990), arranged according to increasing temperature, confronted with *Mg*-number of olivine.

Sample	Rock / texture	Mg/(Mg+Fe) in olivine	T(°C)
F2	pyroxenite/protogranular?	0.91	1052
F1	pyroxenite/protogranular?	0.91	1056
P1	lherzolite/protogranular	0.91	1062
USo	lherzolite/protogranular	0.89	1086
C2v	harzburgite/protogranular	0.92	1089
67	lherzolite/protogranular	0.91	1095
S1v	harzburgite	0.92	1103
S2v	harzburgite	0.92	1113
C1v	herzolite/equigranular	0.92	1124
S4x	lherzolite/porphyroclastic	0.91	1165

tite-quartz (FMQ) buffer (from +0.14 to +0.93 FMQ, Fig. 9) with the exception of harzburgite P4x, which plots one and a half units below FMQ. All samples in Fig. 9 with the exception of P4x lie in the field or very close to the field for slightly metasomatized lherzolites. No sample is of "primitive" character or highly oxidized by metasomatic reactions. The chemical composition of harzburgite P4x is anomalous as it plots outside the fields in Fig. 8, indicating that it is in a state of oxygen disequilibrium. The redox state of porphyroclastic lherzolite S4x indicates equilibrium for the spinel with Cr/(Cr+Al) of 0.26 and disequilibrium for the Cr-rich spinel, with Cr/(Cr+Al) of 0.54.

Discussion

Depletion in xenoliths

The occurrence of upper mantle xenoliths of different lithologies and textural types in a single volcanic vent is a common feature of many volcanic localities worldwide. A depletion process in the mantle is responsible for variations in modal composition, major, minor and trace element contents and different textural types of ultramafic xenoliths. The modal composition of rocks derived from mantle peridotite gradually changes, passing from fertile lherzolites to harzburgites and dunites. The presence of different upper mantle xenoliths in basanite flows of the Kozákov volcano is linked to an inhomogeneity of the upper mantle caused by the extraction of variable volumes of basaltic melt from the primary upper-mantle material.

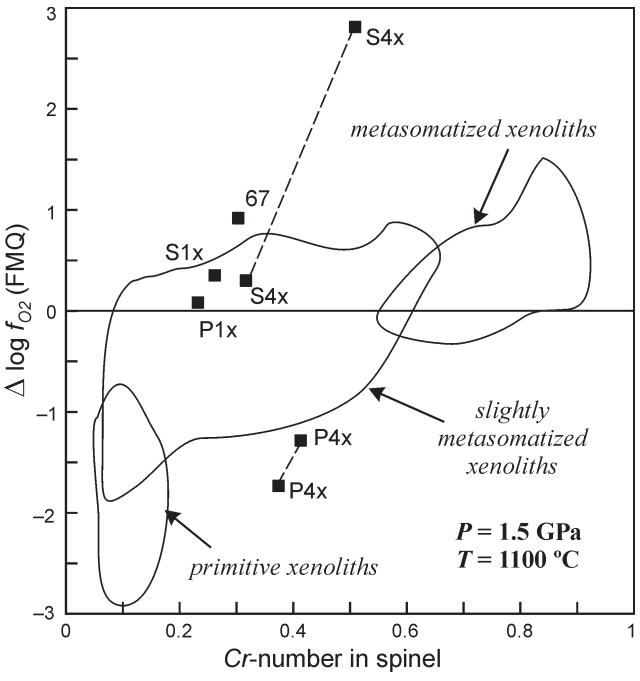

Fig. 9. Deviations of oxygen fugacity from the FMQ buffer plotted against *Cr*-numbers (Cr/Cr+Fe) in spinel. The fields are compiled from many data sources presented by Ballhaus et al. (1991).

However, its possible primary compositional inhomogeneity cannot be completely excluded. The chemical composition of the upper mantle xenoliths and the composition of the constituent minerals is proportional to the degree of partial melting in the Kozákov volcano region: the most abundant are lherzolites, which predominate over harzburgites, together comprising about 96 % of all ultramafic xenoliths; dunites, websterites and pyroxenites are rare (Fediuk 1971). The refractory character is linked with increase in *Mg*-number and decrease in CaO and Al_2O_3 contents. CaO/Al_2O_3 ratios above 1 correspond to lherzolites, and those below 1 to more refractory harzburgites. The lowest TiO_2, Al_2O_3, CaO, Cr_2O_3 contents and the highest MgO contents were recorded in the most residual and refractory dunite. All samples, except for dunites, have MgO contents confined to a small range, being quite far from the primitive mantle. This may indicate either a similar degree of melt extraction and a certain degree of homogeneity in the upper mantle, or similar depths of xenolith entrapment.

Almost all samples have a Ca/Al ratios less than 1.1, characteristic for chondrites (Table 5), indicating a partial melting process, which increases the Ca/Al ratio whereas Al decreases (Palme & Nickel 1985). The lowest Ca/Al ratio indicates the most depleted dunite PAL. If we exclude samples Smrčí (S) and Chuchelna (C), which have extremely high CaO content (Fig. 7) and consequently do not follow the general fractionation trend, then only lherzolite No. 69 has the Ca/Al ratio above 1.1, suggesting an enrichment in clinopyroxene probably by modal metasomatism in the mantle (Stein & Katz 1989).

Variations in modal compositions of the xenoliths are accompanied by changes in chemical compositions of the minerals. Chromium content in spinel is a significant indicator of the depletion process (Bonatti & Michael 1989; Siena et al. 1991). The depletion trend and metasomatic process can be recognized by negatively correlated Al_2O_3 contents in coexisting orthopyroxenes and Cr/(Cr+Al)*100 ratios in spinels, see Fig. 10. The chemical composition of xenoliths, except for porphyroclastic lherzolite S4x (cf. Fig. 10), follow the depletion trend originally defined for conditions of continental passive margins (Bonatti & Michael 1989). The most intensive depletion is exhibited by harzburgite P4x, lying outside the continental lherzolite field (Fig. 10) on an extension toward a higher Cr/(Cr+Al) ratio and a lower Al_2O_3 content in spinel and orthopyroxene, respectively. The most fertile lherzolite is represented by protogranular lherzolite USo.

The compositions of spinel and olivine during progressive melting of lherzolite approach those of Cr-rich spinel and Fo-rich olivine. No trend in terms of $Cr/(Cr+Al+Fe^{3+})$ ratios in spinel and Fo-contents in olivine is evident (Fig. 11), but it may rather follow compositional differences of xenoliths, cf. harzburgite P4x vs. lherzolites (all other samples).

Metasomatic event(s) in the mantle

The process of mantle depletion resulting in geochemical and/or mineralogical changes in upper mantle composition

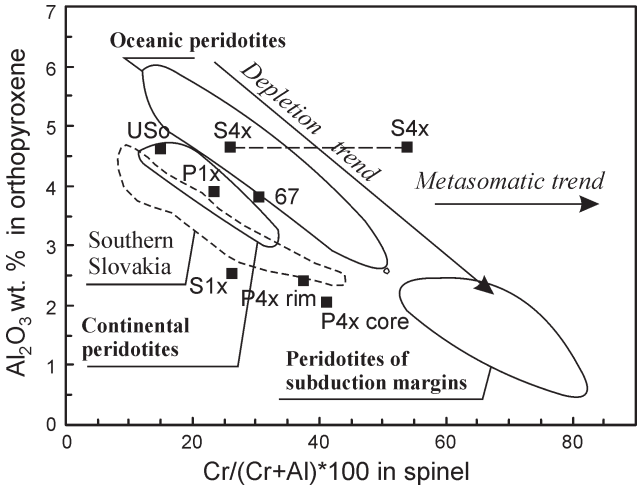

Fig. 10. Compositions of orthopyroxene and spinel of ultramafic xenoliths from the Kozákov volcano in a diagram of Al_2O_3 contents in orthopyroxene vs. Cr/(Cr + Al)*100 ratio in spinel, with trends of depletion and metasomatism. Heavy line fields — oceanic peridotites, continental peridotites and peridotites of subduction margins after Bonatti & Michael et al. (1989), dashed line fields — peridotites from southern Slovakia after Konečný et al. (1995), related to Quaternary alkaline volcanism associated with lithosphere thinning and mantle upwelling during Pliocene–Pleistocene.

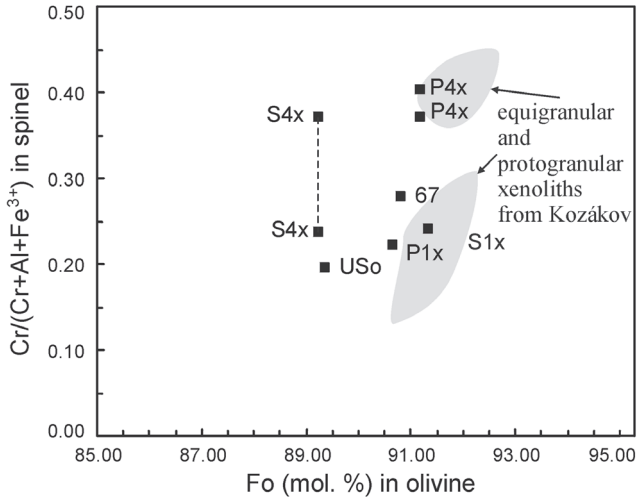

Fig. 11. Cr/(Cr + Al + Fe^{3+}) ratios in spinel vs. Fo contents in olivine. Grey fields represent equigranular and protogranular xenoliths from the Kozákov volcano after Medaris et al. (1999).

is well documented. Metasomatic event(s) caused by reaction between infiltrating agents (melts and/or supercritical fluids) and the mantle rocks are often superimposed on depleted mantle. Previous studies, based on the origin, composition and relation to geotectonic setting, have identified three types of metasomatizing agents: subduction-related fluids (Andersen et al. 1984; Ayers 1998; Zanetti et al. 1999), carbonate melts (Thibault et al. 1992; Ionov et al. 1993; Green & Vallace 1998; Neumann et al. 2002) and mafic silicate melt (Bodinier et al. 1990; Siena et al. 1991; Ionov et al. 1998). The mantle beneath the Kozákov area was located underneath a Cenozoic tectono-volcanic zone, thus we rule out subduction-related fluids. Interaction with carbonatite melt may lead to the formation of wehrlites (Yaxley et al. 1991) or, under different P-T conditions, carbonatite melt may quench in veins or pockets (Ionov et al. 1998) or primary carbonates can crystallize. The Ti/Eu ratio is insensitive to different degrees of partial melting and preserves primitive mantle values of ~7740 (Yaxley et al. 1998). Invasion of carbonatite melt substantially decreases that ratio in peridotite. Mineralogical evidence of carbonatite metasomatism is absent in the Kozákov peridotites, which is consistent with their high Ti/Eu ratio of 6700 for protogranular lherzolite USo and 11500 for protogranular lherzolite 67. The passage of silicate magma through the mantle peridotites is typically accompanied by formation of LREE-enriched amphiboles and/or clinopyroxenes. Silicate magma mostly moves through a system of veins. The intensity of LREE, Sr and Zr enrichment decreases towards the edge of the veins and in the wallrock peridotite it may diminish within some centimeters (Witt-Eickschen et al. 1998). Clinopyroxenite and/or amphibole veins were not observed in the Kozákov xenoliths and modal metasomatism is almost entirely absent. Nevertheless, clinopyroxene and bulk-rock REE patterns (USo protogranular lherzolite) show enrichment in LREE exactly as would be expected for modal metasomatism by silicate melts. LREE enrichment is largely linked to clinopyroxene, but not with newly formed clinopyroxene. Most probably, a pervasive metasomatizing agent penetrated the volume of the peridotite and modified the composition of the original clinopyroxenes. Microscale exchange reactions took place by diffusion over a longer time interval. Such LREE enrichment in clinopyroxene solely by diffusion and/or exchange reaction has been termed "cryptic metasomatism" (Dawson 1984; Picardo et al. 1993; Wiechert et al. 1997).

The U-shape of REE pattern of protogranular xenolith 67 is very similar to those modelled by chromatographic fractionation and reactive porous flow during passage of silicate melts through the peridotite matrix (Navon & Stolper 1987; Takazawa et al. 1992; Nielson & Wilshire 1993; Godard et al. 1995). The melt equilibrates with the peridotite matrix by a diffusion process. Melt percolating for longer distances is selectively enriched in highly incompatible elements due to chromatographic reactions with host peridotite. Changes in the composition of the silicate melt with distance from the melt source, for example a vein system, result in gradation from a steady LREE enriched shape in clinopyroxenes to a U-shape far from the melt source. Either numerical calculations involving 1-D porous flow (constant porosity) or percolative fractionation model (decreasing porosity with distance) can satisfactorily match the REE patterns at various distances from the melt source (Ionov et al. 2002).

The occurrence of two types of spinel (porphyroclastic lherzolite S4x) with significantly different chromium content indicates a bulk metasomatic overprint. The position of high-chromian spinel outside of the general depletion trend and given fields of continental or oceanic peridotites is compatible with a secondary metasomatic origin (cf. Fig. 9).

The observations of cryptic and possible instance of local modal metasomatism, suggests that at least some portions of the mantle beneath Kozákov underwent one or more metasomatic event(s) before fragmentation and entrainment of xenoliths by alkaline magma.

Evolution and conditions

Medaris et al. (1999) and Christensen et al. (2001) presented evidence for a layered structure of the upper mantle beneath the Kozákov volcano area. The structure consists of three horizontal layers, with protogranular lherzolites sandwiched between equigranular lherzolites. The protogranular lherzolite layer spans a depth of 32–70 km. A layered structure of the lithospheric mantle was constrained by comparison of shear-wave splitting of xenoliths and teleseismic observations, which revealed horizontal foliation in the upper equigranular layer, and vertical foliation in the middle protogranular and the lower equigranular mantle layer (Medaris et al. 1999; Christensen et al. 2001). The middle protogranular layer represents a part of a slab of garnet peridotites tectonically emplaced into the upper mantle during Variscan convergent motions (Medaris et al. 1997). Garnet in the protogranular layer became metastable and was replaced by stable spinel-pyroxene symplectite. Thermal conditions in the lithospheric mantle were modified by underplating of the 5 km thick basaltic magma reservoir at 30 Ma age. The shallow upper mantle was heated to higher temperatures and subsequent cooling was faster than in deeper parts.

Although the depth of xenolith extraction cannot be calculated reliably for spinel lherzolite assemblages, we can force the temperature data to fit on a model geotherm of 5 Myr (Medaris et al. 1999). The pressures estimated by such a method give a depth range of 60–80 km. This range is far below the Moho at the present time in N Bohemia (about 32 km — Čermák et al. 1991) and is near the spinel-garnet phase transition boundary (74–92 km).

For the middle protogranular layer, use of the Brey & Köhler (1990) two-pyroxene thermometer, is limited to the temperature range of 850–1090 °C (Medaris et al. 1999). The temperatures of the Kozákov xenoliths arranged in ascending order (1052–1165 °C) indicate that most samples refer to the lower part of the protogranular slab and a few high-temperature samples correspond to the underlying equigranular layer. Samples corresponding to the upper equigranular layer are absent. The highest temperatures are recorded in samples containing Al-rich coexisting pyroxenes (Fig. 4).

The *Mg*-numbers of olivine (90.6–91.8) tend to increase with temperature and pressure, defining a trend of progressive depletion with depth. Medaris et al. (1999) have reported an exactly opposite correlation, suggesting that no straightforward relation exists between depth and degree of depletion.

In regions with strong metasomatic overprint, the oxygen fugacity is raised above the FMQ buffer up to +3 log units (Ballhaus et al. 1991; Amundsen & Neumann 1992). The oxidation state of the upper mantle beneath the Kozákov volcano was slightly above the FMQ buffer (from +0.14 to +0.93 log unit), which compares well with the oxygen fugacity for the subcontinental lithospheric mantle ($+0.24 \pm 0.5$) from the classical localities of the world (Massif Central, Kilbourne Hole, San Carlos, Central Asia — Wood & Virgo 1989; Bryndzia & Wood 1990). The oxidation state of the mantle beneath the Kozákov volcano implies a restricted role for modal metasomatism. On the contrary, the presence of Cr-rich spinels ($Cr/(Cr+Al) > 0.5$) is most probably the result of increased temperature during metasomatism, but the rare occurrence of these spinels decreases the significance of this process. The cryptic metasomatism has a negligible effect on the calculation of oxygen fugacity.

Two processes considered to promote $Cr/(Cr+Al)$ ratio in spinel are depletion and metasomatism. The harzburgite P4x is relatively reduced but has high $Cr/(Cr+Al)$ ratio in spinel (Fig. 8) and additionally is the most depleted xenolith. Increased chromium in spinel may be the result of more intensive depletion than in the majority of the non-metasomatized peridotites (Fig. 8).

Protogranular lherzolite USo shows evidence of exposure to bulk cryptic metasomatism. According to the equilibrium temperature of this xenolith (1086 °C), it originates from the bottom part of the protogranular mantle layer, which was not thermally affected by Cenozoic rifting (Medaris et al. 1999). Cryptic metasomatism requires a longer time to change the composition of the clinopyroxenes, compared to flow infiltration of melt through a vein system reacting directly with the surrounding mantle. Diffusion model calculations of reaction between metasomatizing melt and clinopyroxene, modifying the inherited LREE-depleted to an LREE-enriched pattern, imply that complete re-homogenization of a 1 mm crystal takes up to 16 kyr (Beccaluva et al. 2001). By contrast, amphibole in peridotite adjacent to a metasomatizing melt may attain the observed diffusion profile in a period of not longer than 10–15 years (Witt-Eickschen et al. 1998). The effectiveness of liquid-solid diffusion reactions may imply the occurrence of metasomatic reactions a short time before the xenolith entrainment in the host basalt (Witt-Eickschen et al. 1998; Wulf-Pedersen et al. 1999). A much slower process(es) for cryptic metasomatism may be expected, as a much smaller volume is involved in reaction with the mantle peridotite. It has been suggested that the metasomatizing magmas are to be derived from the deep asthenospheric mantle (Schiano & Clocchiatti 1994; Vaselli et al. 1995; Witt-Eickschen et al. 1998).

Protogranular lherzolite 67, according to temperature 1095 °C, is located at the boundary between the protogranular and underlying equigranular mantle layer (Medaris et al. 1999). The U-shaped REE pattern of protogranular lherzolite 67 is intrepreted as consequence of cryptic metasomatism of highly fractionated silicate melts with the host peridotite. Melt enriched in incompatible elements can be evolved over relatively short distances (Zanetti et al. 1996), but Nielson & Wilshire (1993) argue for long percolation paths necessary for effectiveness of the chromatographic fractionation. A single event modelled by

reactive porous flow can explain the majority of both types of REE patterns in clinopyroxenes (LREE enriched and U-shaped) in the Spitsbergen mantle. The process operated beneath the volcanic area on a scale of several kilometers involving a large portion of the lithospheric mantle (Ionov et al. 2002). A large scale modal metasomatic event in the mantle beneath the Quaternary West Eifel Volcanic Field, Germany, led to the formation of secondary amphibole, clinopyroxene and phlogopite during the Variscan orogeny (Shaw et al. 2005). A younger event, related to Quaternary volcanism, is characterized by amphibole-phlogopite-clinopyroxene veins (Shaw et al. 2005).

The similar depth of protogrnanular xenoliths USo and 67 cannot be an argument for a large scale pervasive metasomatism in the lithospheric mantle under Kozákov. Both xenoliths come from middle protogranular mantle layer, defined by Medaris et al. (1999), intensively affected during the Variscan orogeny. The astenospheric metasomatizing melts could have been generated during the Variscan orogeny, when initial collisional movements were followed by post-thickening extension, which resulted in uplift of the protogranular mantle layer to the recent position. Either the protograular mantle layer was metasomatized prior to final emplacement or synchroneously with uplift, alternatively a certain short time after uplift.

Arguments against the Neogene metasomatizing event are: (1) gross mantle structure related most likely to the Variscan tectonics (Christensen et al. 2001), (2) negligible Neogene reheating of the protogranular mantle layer to promote diffusion metasomatic reactions, (3) a relatively short period of mantle relaxation after uderplating and hence possible time for infiltration of deep astenospheric melts, (4) absence of clinopyroxene-amphibole ± phlogopite veins, hosted by peridotite, associated with passage of silicate melts during Quaternary volcanism.

Conclusions

The ultramafic xenoliths from the Kozákov volcano represent a deeper part of a layered uppermost mantle as described by Medaris et al. (1999) and Christensen et al. (2001). Specifically the xenoliths correspond to the lower half of the protogranular layer and to the underlying equigranular layer, comprising a depth range of 50–75 km and a temperature interval of 1165–1052 °C. This deeper mantle shares features of subcontinental mantle, deduced from mineral compositions and oxygen fugacities clustered slightly above the FMQ buffer (from +0.14 to +0.93 FMQ). The bulk-rock major element chemistry points to a similar degree of depletion in the xenoliths, indicating a coherent evolution of the Kozákov upper mantle. The degree of depletion is sufficiently advanced and ubiquitous for no single sample to approach the composition of the primitive mantle. Subordinate dunites and wehrlites are associated with mantle inhomogeneity.

The presence of two spinel types with low and high Cr content in only one xenolith and absence of typical metasomatic minerals like amphiboles, clinopyroxenes or phlogopites suggests negligible involvement of bulk metasomatism. The LREE enriched pattern in clinopyroxenes from protogranular lherzolites USo and the U-shaped REE pattern in clinopyroxenes from protogranular lherzolites 67 reveal a modification of LREE, which cannot be explained by melt extraction but requires involvement of cryptic metasomatic process(es). The exact age of the metasomatic event(s) is unknown, but may have occurred in pre-Neogene time, possibly in association with the late Variscan development of the Bohemian Massif.

We conclude that, although there is very scant evidence of modal metasomatism on a macro/micro scale, the REE patterns in clinopyroxene and the bulk rock compositions reflect cryptic metasomatic changes at least in some deeper parts of the subcontinental mantle beneath Kozákov.

Acknowledgments: Financial support for this research was provided by Project A3013403 of the Grant Agency of the Academy of Sciences of the Czech Republic, the Scientific Programme CEZ: Z3-013-912 of the Institute of Geology, AS CR, and subsidiary also from the VEGA Grant No. 1/1029/04. The authors gratefully acknowledge L.G. Medaris, Wisconsin, H.G. Stosh, Köln am Rhein, and F.E. Lloyd, Bristol for their stimulating comments, and E. Jelínek for providing unpublished data on xenoliths from Kozákov. We thank O. Vaselli, Florence, Cs. Szabo, Budapest and J. Lexa, Bratislava for their comments.

References

Amundsen H.E.F. & Neumann E.R. 1992: Redox control during mantle/melt interaction. *Geochim. Cosmochim. Acta* 56, 2405–2416.

Andersen T., O'Reily S.Y. & Griffin W.L. 1984: The trapped fluid phase in upper mantle xenoliths from Victoria, Australia: implications for mantle metasomatism. *Contr. Mineral. Petrology* 88, 72–85.

Ayers J. 1998: Trace elements modeling of aqueous fluid — peridotite interaction in the mantle wedge of subduction zones. *Contr. Mineral. Petrology* 132, 390–404.

Babuška V. & Plomerová J. 1988: Subcrustal continental lithosphere: a model of its thickness and anisotropic structure. *Phys. Earth Planet. Inter.* 51, 130–132.

Ballhaus C., Berry R.F. & Green D.H. 1991: High pressure experimental calibration of olivine-orthopyroxene-spinel oxygen geobarometer: implications for the oxidation state of the upper mantle. *Contr. Mineral. Petrology* 107, 27–40.

Beccaluva L., Bonadiman C., Coltorti M., Salvini L. & Siena F. 2001: Depletion events, nature of metasomatizing agent and timing of enrichment processes in lithospheric mantle xenoliths from the Veneto Volcanic Province. *J. Petrology* 42, 1, 173–187.

Bellon H. & Kopecký L. 1977: Spectres d'ages radiométriques du volcanisme du rift du Massif Bohémien. *5eme Réunion Ann. Sci. Terre, Rennes, Soc. Géol. Fr. éd.* 57.

Bodinier J.L., Vasseur G., Verniéres J., Dupuy C. & Fabriés J. 1990: Mechanisms of mantle metasomatism: geochemical evidence from Lherz orogenic massif. *J. Petrology* 31, 597–628.

Bonatti E. & Michael J. 1989: Mantle peridotites from continental rifts to ocean basins to subduction zones. *Earth Planet. Sci. Lett.* 91, 297–311.

Brey G.P. & Köhler T. 1990: Geothermobarometry in four-phase lherzolites II. New thermobarometers, practical assessment of existing thermobarometers. *J. Petrology* 31, 1353–1378.

Bryndzia L.T. & Wood B.J. 1990: Oxygen thermobarometry of abyssal spinel peridotites: the redox state and C-O-H volatile composition of the Earth's suboceanic upper mantle. *Amer. J. Sci.* 290, 1093–1116.

Čermák V.M., Král M., Kubík J. & Šafanda J. 1991: Heat flow, regional geophysics and lithosphere structure in Czechoslovakia and adjacent part of Central Europe. In: Čermák V. & Rybach L. (Eds.): Terrestrial heat flow and lithosphere structure. *Springer-Verlag,* Berlin, 133–165.

Christensen N.I., Medaris I.G., Wang H.F. & Jelinek E. 2001: Depth variation of seismic anisotropy and petrology in central European lithosphere: A tectonothermal synthesis from spinel lherzolite xenoliths. *J. Geophys. Res.* 106, 645–664.

Dawson J.B. 1984: Contrasting types of upper mantle metasomatism. In: Kornprobst J. (Ed.): Kimberlites. II. The mantle and crust-mantle relationships. *Elsevier,* Amsterdam, 289–294.

Downes H. 2001: Formation and modification of the shallow subcontinental lithospheric mantle: a review of geochemical evidence from ultramafic xenolith suites and tectonically emplaced ultramafic massifs of Western and Central Europe. *J. Petrology* 42, 233–250.

Downes H. & Dupuy C. 1987: Textural, isotopic and REE variations in spinel peridotite xenoliths, Massif Central, France. *Earth Planet. Sci. Lett.* 82, 121–135.

Downes H., Embey-Isztin A. & Thirlwall M. 1992: Petrology and geochemistry of spinel peridotite xenoliths from western Pannonian Basin (Hungary): evidence for an association between enrichment and texture in the upper mantle. *Contr. Mineral. Petrology* 109, 340–354.

Erickson S.C., Fourie P.J. & De Jager D.H. 1985: A cumulate origin for the minerals in clinopyroxenites of the Phalaborwa Complex. *Trans. Geol. Soc. S. Africa* 88, 207–214.

Farský F. 1876: Mineralogische Notizen I. Mineralien aus der Kosakover Basaltkugeln. *K.-kön. Geol. Reichsanst, (Wien)* 205–208.

Fediuk F. 1968: Additional notes on the basaltic volcanics and their ultrabasic nodules at Smrčí in the Železný Brod area. *Fac. Sci. Charles Univ.,* Praha, 1–12 (in Czech).

Fediuk F. 1971: Ultramafitites in the area of the Krkonoše–Jizerské hory Mountains. *Acta Univ. Carol., Geol.* 319–343 (in Czech).

Fediuk F. & Fediuková E. 1989: Ultramafic nodules in basalts from northern Moravia, Czechoslovakia. *Sbor. Geol. Věd, Ř. Geol.* 44, 4–49.

Frýda J. & Vokurka K. 1995: Evidence for carbonatite metasomatism in the upper mantle beneath the Bohemian Massif. *J. Czech Geol. Soc.* 43, A–9–10.

Godard M., Bodinier J.L. & Vasseur G. 1995: Effects of mineralogical reactions on trace element redistributions in mantle rocks during percolation process: a chromatographic approach. *Earth Planet. Sci. Lett.* 133, 449–461.

Green D.H. & Vallace M.E. 1998: Mantle metasomatism by ephemeral carbonatite melts. *Nature* 336, 459–462.

Ionov D.A. 1998: Trace element composition of mantle-derived carbonates and coexisting phases in peridotite xenoliths from alkali basalts. *J. Petrology* 39, 1931–1941.

Ionov D.A., Dupuy C., O'Reily S.Y., Kopylova M.G. & Genshaft Yu.S. 1993: Carbonated peridotite xenoliths from Spitsbergen: implications for trace element signature of mantle carbonate metasomatism. *Earth Planet. Sci. Lett.* 119, 283–297.

Ionov D.A., Bodinier J.L., Mukasa S.B. & Zanetti A. 2002: Mechanisms and sources of mantle metasomatism: major and trace element compositions of peridotite xenoliths from Spitsbergen in the context of numerical modelling. *J. Petrology* 43, 2219–2259.

Jakeš P. & Vokurka K. 1987: Central Europe. In: Nixon P.H. (Ed.): Mantle xenoliths. Chichester, 149–154.

Köhler T.P. & Brey G.P. 1990: Calcium exchange between olivine and clinopyroxene calibrated as geothermobarometer for natural peridotites from 2 to 60 kb with applications. *Geochim. Cosmochim. Acta* 54, 2375–2388.

Konečný P., Konečný V., Lexa J. & Huraiová M. 1995: Mantle xenoliths in alkali basalts of southern Slovakia. *Acta Vulcanol.* 7, 2, 241–247.

Konečný P., Huraiová M. & Bielik M. 1999: P-T-X-fO_2 conditions in upper mantle: evidence from lherzolitic xenoliths hosted by Plio-Pleistocene alkali basalts. *Geolines* 9, 59–66.

Konzalová M. 1973: Neogene plant microsossils of river sediments from underground of the Neoidic volcanites of the Železný Brod area. *Věst. Ústř. Úst. Geol.* 48, 17–23 (in Czech).

Kopecký P. 1968: Geological map of the territory between Železný Brod, Semily and Kozákov. *Unpublished MSc Thesis, Charles University,* Prague 1–88 (in Czech).

Kramer W. & Seifert W. 2000: Mafische Xenolithe und Magmatite im östlichen Saxothuringikum und westlichen Lugikum: Ein Beitrag zum Krustenbau und zur regional Geologie. *Z. Geol. Wiss.* 28, 133–156.

Lenoir X., Garrido C.J., Bodinier J.L. & Dautria J.M. 2000: Contrasting lithospheric mantle domains beneath the Massif Central (France) revealed by geochemistry of peridotite xenoliths. *Earth Planet. Sci. Lett.* 181, 359–375.

Le Maitre R.W. (Ed.) 2002: Igneous rocks. A classification and glossary of terms. 2nd Edition. *Cambridge University Press,* Cambridge, 1–236.

Lloyd F.E. 1987: Characterization of mantle metasomatic fluids in spinel lherzolites and alkali clinopyroxenites from the West Eifel and South Uganda. In: Menzies M.A. & Hawkesworth C.J. (Eds.): Mantle metasomatism. *Academic Press,* London, 91–120.

Lloyd F.E. & Bailey D.K. 1975: Light element metasomatism of the continental mantle: the evidence and the consequences. *Phys. Chem. Earth* 9, 389–416.

Lloyd F.E. & Bailey D.K. 1994: Complex mineral textures in bebedourite: possible links with alkali clinopyroxenite xenoliths and kamafugite volcanism. In: Mayer O.H.A. & Leonardos O.H. (Eds.): Proceed. 5th Intern. Conf. Vol. I. Kimberlites. Related rocks and mantle xenoliths. *CPRM Spec. Publ.,* Rio de Janeiro, Brazil, 263–269.

Luhr J.F. & Aranda-Gómez J.J. 1997: Mexican peridotite xenoliths and tectonic terranes: correlations among vent location, texture, temperature, pressure and oxygen fugacity. *J. Petrology* 38, 2, 1075–1112.

McDonough W.F., Stosch H.S. & Ware N.G. 1992a: Distribution of titanium and the rare earth elements between peridotitic minerals. *Contr. Mineral. Petrology* 110, 321–328.

McDonough W.F., Sun S.S. Ringwood A.E. Jagoutz E. & Hofmann. A.W. 1992b: Potassium, rubidium, and cesium in the Earth and Moon and the evolution of the mantle of the Earth. *Geochim. Cosmochim. Acta.* 56, 1001–1012.

Medaris L.G. (Jr.), Fournelle J.H., Wang H.F. & Jelínek E. 1997: Thermobarometry and reconstructed chemical compositions of spinel-pyroxene symplectites: evidence for pre-existing garnet in lherzolite xenoliths from Czech Neogene lavas. *Russian Geol. Geophys.* 38, 277–286.

Medaris L.G. (Jr.), Wang H.F., Fournelle J.H., Zimmer J.H. & Jelínek E. 1999: A cautionary tale of spinel peridotite thermobarometry: an example from xenoliths of Kozákov volcano, Czech Republic. *Geolines* 9, 92–95.

Menzies M.A., Kempton P.D. & Dugan M.A. 1985: Interaction of continental lithosphere and asthenospheric melts below the Geronimo volcanic field, Arizona, U.S.A. *J. Petrology* 26, 663–693.

Mercier J.C. & Nicolas A. 1975: Textures and fabrics of upper-mantle peridotites as illustrated by xenoliths from basalts. *J. Petrology* 16, 454–487.

Mihaljevič M. 1993: Geochemistry of olivine-free ultramafic nodules from the České středohoří Mts. *Ph.D. Thesis Charles University,* Prague, 1–112 (in Czech).

Navon O. & Stolper E. 1987: Geochemical consequences of melt percolation: the upper mantle as chromatographic column. *J. Geol.* 95, 285–307.

Neumann E.R., Wulf-Pedersen E., Pearson N.J. & Spencer E.A. 2002: Mantle xenoliths from Tenerife (Canary Islands): evidence for reactions between mantle peridotites and silicic carbonatite melts including Ca metasomatism. *J. Petrology* 43, 825–857.

Nielson J.E. & Wilshire H.G. 1993: Magma transport and metasomatism in the mantle: a critical review of current geochemical models. *Amer. Mineralogist* 78, 1117–1134.

O'Neill H.S.T. 1981: The transition between spinel lherzolite and garnet lherzolite, and its use as a geobarometer. *Contr. Mineral. Petrology* 77, 185–194.

Palme H. & Nickel K.G. 1985: Ca/Al ratio and composition of the Earth's upper mantle. *Geochim. Cosmochim. Acta* 49, 2123–2132.

Parkinson I.J. & Pearce J.A. 1998: Peridotites from the Izu-Bonin-Mariana forearc (ODP Leg 125): evidence for mantle melting and melt-mantle interaction in a supra-subduction zone setting. *J. Petrology* 39, 9, 1577–1618.

Piccardo G.B., Rampone E., Vannucci R., Shimizu N., Ottolini L. & Bottazzi P. 1993: Mantle processes in the sub-continental lithosphere: the case study of the rifted sp-lherzolites from Zabargad (Red Sea). *Europ. J. Mineral.* 5, 1039–1056.

Plomerová J., Babuška V. & Horálek J. 1998: Seismic anisotropy and velocity variation in the mantle beneath the Saxothuringicum-Moldanubicum contact in Central Europe. *Pure Appl. Geophys.* 151, 365–394.

Schiano P. & Clocchiatti R. 1994: Worldwide occurrence of silica-rich melts in sub-continental and sub-oceanic mantle minerals. *Nature* 368, 621–623.

Schovánek P. 1977: Petrology of selected ultramafic rocks of the Bohemian Masssif and chemical composition of their minerals. *Unpublished PhD Thesis, Charles University,* Prague 1–88 (in Czech).

Shaw S.J., Eyzaguirre J., Fryer B. & Gagnon J. 2005: Regional variations in the mineralogy of metasomatic assemblages in mantle xenoliths from the West Eifel Volcanic Field, Germany. *J. Petrology* 5, 945–972.

Šibrava V. & Havlíček P. 1980: Radiometric age of Plio-Pleistocene volcanic rocks of the Bohemian Massif. *Věst. Ústř. Úst. Geol.* 55, 129–139.

Siena F. & Coltorti M. 1993: Thermobarometric evolution and metasomatic processes of upper mantle in different tectonic settings: evidence from spinel peridotite xenoliths. *Europ. J. Mineral.* 5, 1073–1090.

Siena F., Beccaluva L., Coltorti M., Marchesi S. & Morra V. 1991: Ridge hot-spot evolution of the Atlantic lithospheric mantle: evidence from Lanzarote peridotite xenoliths (Canary Islands). *J. Petrology, Spec. Lherzolites Issue,* 271–290.

Stein M. & Katz A. 1989: The composition of subcontinental lithosphere beneath Israel: inferences from peridotitic xenoliths. *Israel J. Earth Sci.* 38, 75–87.

Stosh H.G. & Lugmair G.W. 1986: Trace elements and Sr and Nd isotope geochemistry of peridotite xenoliths from Eifel (W Germany) and their bearing on the evolution of the sub-continental lithosphere? *Earth Planet. Sci. Lett.* 80, 281–298.

Stosh H.G., Lugmair G.W. & Kovalenko V.I. 1986: Spinel peridotite xenoliths from the Tariat Depression, Mongolia. II: Geochemistry and Sr isotopic trace elements and Nd a and Sr isotopic composition and their implications for the evolution of the sub-continental lithosphere. *Geochim. Cosmochim. Acta* 50, 2601–2614.

Streckeisen A. 1979: Classification and nomenclature of volcanic rocks, lamprophyres, carbonatites and melilitic rocks: recommendations and suggestions of the IUGS subcommision on the systematics of igneous rocks. *Geology* 7, 331–335.

Sun S.S. 1982. Chemical composition and origin of the Earth's primitive mantle. *Geochim. Cosmochim. Acta* 46, 179–192.

Takazawa E., Frey F.A., Shimizu N., Obata M. & Bodinier J.L. 1992: Geochemical evidence form melt migration and reaction in the upper mantle. *Nature* 359, 55–58.

Taylor S.R. & McLennan F. 1985: The continental crust: its composition and evolution. *Blackwell,* Oxford, 1–379 (in Russian).

Thibault Y., Edgar A. & Lloyd F. 1992: Experimental investigation of melts from a carbonated phlogopite lherzolite: implications for metasomatism in continental lithospheric mantle. *Amer. Mineralogist* 77, 784–794.

Ulrych J. & Pivec E. 1997: Age-related contrasting alkaline volcanic series in North Bohemia. *Chemie Erde* 57, 311–336.

Ulrych J., Kopecký L. & Kropáček V. 1991(Eds.): Guide to Post-symposium excursion: Neoidic volcanism of the Bohemian Massif. *June 27 to 29, 1991, Charles University* 1991, 1–58.

Ulrych J., Lloyd F.E., Balogh K., Hegner E., Langrová A., Lang M., Novák J.K. & Řanda Z. 2005: Petrogenesis of alkali pyroxenite and ijolite xenoliths from the Tertiary Loučná–Oberwiesenthal Volcanic Centre, Bohemian Massif in the light of new mineralogical, geochemical and isotopic data. *Neu. Jb. Mineral., Abh.* 182, 57–79.

Ulrych J., Pivec E., Lang M., Balogh K. & Kropáček V. 1999: Cenozoic intraplate volcanic series in of the Bohemian Massif: a review. *Geolines* 9, 123–129.

Ulrych J., Pivec E., Povondra P. & Rutšek J. 2000: Upper-mantle xenoliths in melilitic rocks of the Osečná complex, North Bohemia. *J. Czech Geol. Soc.* 45, 1–15.

Upton B.G.J. 1967: Alkaline pyroxenites. In: Wyllie P.J. (Ed.): Ultramafic and related rocks. *J.Wiley,* New York, 281–288.

Vaselli O., Downes H., Thirlwall M., Dobosi G., Coradossi N., Seghedi I., Szakacs A. & Vannucci R. 1995: Ultramafic xenoliths in Plio-Pleistocene alkali basalts from Eastern Transylvanian Basin: Depleted mantle enriched by vein metasomatism. *J. Petrology* 36, 1, 23–53.

Vokurka K. 1979: The study of elements equilibrium between minerals of ultramafic xenoliths of the Kozákov volcano. *Unpublished MSc Thesis, Charles University,* Prague (in Czech).

Vokurka K. & Kober B. 1993: Heterogeneity of the Earth's mantle below the Bohemian Massif. In: Kukal Z. (Ed.): Proceedings of the 1st International Conference on the Bohemian Massif, Prague, Czechosl. Sept. 26–Oct. 3, 1988. *Czech Geol. Surv.,* Prague, 327–330.

Vokurka K. & Povondra P. 1983: Geothermometry and geobarometry of lherzolite nodules from Kozákov, NE Bohemia, Czechoslovakia. *Acta Univ. Carol., Geol.* 261–272.

Wass S.Y. & Rogers N.W. 1980: Mantle metasomatism — precursor to continental alkaline volcanism. *Geochim. Cosmochim. Acta* 44, 1811–1823.

Webb S.A.C. & Wood B.J. 1986: Spinel-pyroxene-garnet relationships and their dependence on Cr-Al ratio. *Contr. Mineral. Petrology* 92, 471–480.

Wedepohl K.H. 1987: Kontinentaler Intraplatten-Vulkanismus am Beispiel der tertiären Basalte der Hessischen Senke. *Fortschr. Mineral.* 65, 19–47.

Wedepohl K.H., Gohn E. & Hartmann G. 1994: Cenozoic alkali basaltic magmas of western Germany and their products of differentiation. *Contr. Mineral. Petrology* 115, 253–278.

Wiechert U., Ionov D.A. & Wedepohl K.H. 1997: Spinel peridotite xenoliths from the Atsagin-Dush volcano, Dariganga lava plateau, Mongolia: A record of partial melting and cryptic metasomatism in the upper mantle. *Contr. Mineral. Petrology* 126, 346–367.

Wilshire H.G., Nielson Pike J.E., Mayers C.E. & Schwarzmann E.C. 1980: Amphibole rich veins in lherzolite xenoliths, Dish Hill and Deadman Lake, California. *Amer. J. Sci.* A280, 576–593.

Wilson M. & Downes H. 1991: Tertiary-Quaternary extension-related alkaline magmatism in western and central Europe. *J. Petrology* 32, 811–850.

Wilson M., Rosenbaum J. & Ulrych J. 1994: Cenozoic magmatism of the Ohře rift, Czech Republic: geochemical signatures and mantle dynamics. *Abst. Int. Volcanol. Congress,* Ankara 1.

Witt-Eickschen G. 1993: Upper mantle xenoliths from alkali basalts of the Vogelsberg, Germany: implications for mantle upweling and metasomatism. *Eur. J. Mineral.* 5, 361–376.

Witt-Eickschen G. & Kramm U. 1998: Evidence for the multiple stage evolution of the subcontinental lithospheric mantle beneath the Eifel (Germany) from pyroxenite and composite pyroxenite/peridotite xenoliths. *Contr. Mineral. Petrology* 131, 258–272.

Witt-Eickschen G., Kaminsky W., Kramm U. & Harte B. 1998: The nature of young vein metasomatism in the lithosphere of the West Eifel (Germany): geochemical and isotopic constraints from composite mantle xenoliths from the Meerfelder Maar. *J. Petrology* 34, 155–185.

Wood B.J. & Virgo D. 1989: Upper mantle oxidation state: ferric iron contents of lherzolite spinels by ^{57}Fe Mössbauer spectroscopy and resultant oxygen fugacities. *Geochim. Cosmochim. Acta* 53, 1277–1291.

Wulf-Pedersen E., Neumann E.R., Vanucci R., Bottazzi P. & Ottolini L. 1999: Silicic melts produced by reaction between peridotite and infiltrating basaltic melts: ion probe data on glasses and minerals in veined xenoliths from La Palma, Canary Islands. *Contr. Mineral. Petrology* 137, 59–82.

Xu Y., Menzies M.A., Vroon P., Mercier J.C. & Lin C. 1998: Texture-temperature-geochemistry relationships in the upper mantle as revealed from spinel peridotite xenoliths from Wangquing, NE China. *J. Petrology* 39, 469–493.

Yaxley G.M., Crawford A.J. & Green D.H. 1991: Evidence for carbonatite metasomatism in spinel peridotites from western Victoria, Australia. *Earth Planet. Sci. Lett.* 197, 305–317.

Yaxley G.M., Green D.H. & Kamenetsky V. 1998: Carbonatite metasomatism in the Southeastern Australian lithosphere. *J. Petrology* 39, 11, 12, 1917–1930.

Zanetti A., Vannucci R., Oberti P. & Ottolini L. 1996: Infiltration metasomatism at Lherz as monitored by systematic ion-microprobe investigations close to a hornblendite vein. *Chem. Geol.* 134, 113–133.

Zanetti A., Mazzucchelli M., Rivalenti G. & Vannucci R. 1999: The Finero phlogopite-peridotite massif: an example of subduction-related metasomatism. *Contr. Mineral. Petrology* 134, 107–122.